9-1-2024

Understanding the Mystery of R-Loops and Their Relationship to Nucleolar Stress

Kevin Shane
Loyola University of Chicago Graduate School

LOYOLA UNIVERSITY CHICAGO

UNDERSTANDING THE MYSTERY OF R-LOOPS AND THEIR RELATIONSHIP TO NUCLEOLAR STRESS

A THESIS SUBMITTED TO

THE FACULTY OF THE GRADUATE SCHOOL

IN CANDIDACY FOR THE DEGREE OF

MASTER OF SCIENCE

PROGRAM IN INTEGRATIVE CELL BIOLOGY

BY

KEVIN SHANE

CHICAGO, ILLINOIS

AUGUST 2024

ACKNOWLEDGEMENTS

Thank you to my committee for giving me their time and effort to improve my way of thinking about science. My program director, Dr. Phong Le, was a welcoming and helpful presence throughout my time at Loyola. I would specifically like to thank Dr. Weihang Chai for allowing me to join her lab, her dedication in improving my science, and general advice about life. I would also like to thank the members of the Chai lab for their constant support and advice. They were always extremely friendly to me and gracious in answering any question I had. A special thank you to the administrative director of student academics and wellness, Anna Sofinski (Dauzvardis). Anna went above and beyond to help me every step of the way in the thesis process. Also, my friends from Loyola were a great support system and made pursuing this masters degree a great experience. Lastly, I would like to thank my family for supporting me, and putting up with me, during this process.

TABLE OF CONTENTS

LIST OF TABLES

LIST OF FIGURES

LIST OF ABBREVIATIONS

SETX Senataxin
RNAPII Ribonucleic Polymerase II
DNA Deoxyribonucleic acid
ds Double stranded
dsDNA Double stranded deoxyribonucleic acid
DSB Double strand breaks
Lnc Long non-coding
FC Fibrillar center
DFC Dense fibrillar center
GC Granular component
MDM2/4 Mouse double murine 2/4
HDM2 Human double murine 2
AML Acute Myeloid Leukemia
HOXA Homeobox A cluster
BRD4 Bromodomain-containing Protein 4
ATR Ataxia telangiectasia and Rad3-related protein
CHK1 Checkpoint kinase 1
RNA Ribonucleic acid
DRIP DNA-RNA immunoprecipitation
NPM1 Nucleophosmin 1
HBD-EGFP Hybrid-enhanced green fluorescent protein
HDM2 Human double murine 2
PFA Paraformaldehyde
HRP Horseradish peroxidase
mL Milliliter
PBS Phosphate buffered saline
PBST Phosphate buffered saline tween
IF Immunofluorescence
U2OS Human osteosarcoma cell line
GAPDH Glyceraldehyde-3-phosphate dehydrogenase
MDA-MB-231 Triple negative breast cancer cell line
Act. D. Actinomycin D.
MTT 3-(4,5-dimethylthiazolyl-2)-2,5-diphenyltetrazolium bromide
MMC Mitomycin C
TRC Transcription replication conflict
siRNA Small interfering RNA

ABSTRACT

Genomic instability is an increase in the likelihood of DNA mutations and genetic changes during cell division, a common feature in cancer cells. One cause of genomic instability comes from the aberrant formation of three-stranded nucleic acid structures called R-loops. R-loop form when an RNA strand hybridizes to its complementary strand of DNA, forming a stable RNA:DNA hybrid and displacing one free strand of DNA [1]. Accumulation of unscheduled R-loops can lead to replication stress, fork collision, gene expression changes, and double-strand breaks that are underlying causes of genome instability and the development of many diseases, including cancer [2]. Many cancers, such as breast, lung, ovarian, and prostate, have all been found to have an accumulation of R-loops [3].

The nucleolus is a membrane-less organelle inside the nucleus. It is where ribosomal DNA (rDNA) transcription, ribosomal RNA (rRNA) modification, and assembly of ribosomes occur [4]. This is the most energetically intensive process in the cell [4,5]. In cancer cells, nucleoli are typically increased in size and/or number due to the increased protein production a cancer cell needs to survive, a sign of poor prognosis in many cancer types [6,7]. The nucleolus is also a sensor of cellular or genomic stress and can induce p53 activation upon stress [8].

Due to the high volume of transcription occurring in the nucleolus, it is likely that a well-regulated R-loop homeostasis is important to the proper functioning of the nucleolus. While it is well known that the nucleolus responds to a vast array of stressors, it is currently unknown if an increase in genomic R-loops can cause nucleolar stress. I hypothesize that increasing R-loop abundance in cells will cause nucleolar stress. In addition, increasing R-loop abundance will

sensitize cancer cells to DNA damage inducing or DNA repair inhibiting chemotherapeutic agents. I tested this hypothesis with the following aims.

Aim 1. Determine whether DNA damaging or DNA repair inhibiting chemotherapeutic agents affect R-loop abundance and localization in the nucleus

I hypothesized that the addition of DNA damage inducing or DNA repair inhibiting chemotherapeutic agents would alter R-loop abundance and localization in cells. My results show that selected DNA damage inducing or DNA repair inhibiting chemotherapeutic agents including Cisplatin and Olaparib slightly increase the abundance of R-loops in cells, but none of the tested chemotherapeutic agents alter the relative location of R-loops in the nucleus.

Aim 2. Determine whether R-loops are concentrated in the nucleolus and whether increasing the abundance of R-loops can activate the nucleolar stress pathway

I hypothesized that R-loops were concentrated in the nucleolus, and increasing R-loops would activate the nucleolar stress pathway. My immunostaining results show that R-loops appear to be concentrated in the nucleolus and increasing R-loop abundance in cells partially activates the nucleolar stress pathway.

Aim 3. Determine whether increasing R-loop levels decreases cell viability

I hypothesized that increasing R-loop levels with an addition of DNA damaging, and DNA repair inhibiting drugs and knockdown of Senataxin would activate the nucleolar stress pathway leading to a decrease in cell viability. Unfortunately, no reliable data could be

gathered from this aim. The results in this aim were unreliable due to an inconsistent cell counting method and low cell seeding density.

CHAPTER ONE

BACKGROUND AND RATIONALE OF THE RESEARCH

How R-loops Form

The R-loop in its basic form is a three-stranded structure that occurs when an RNA strand hybridizes to its complementary DNA strand. The binding of the newly transcribed nascent RNA strand to its complimentary DNA strand causes the displacement of the unbound DNA strand, forming a three stranded structure in the genome (Figure 1). R-loops are typically found in G-C rich and transcriptionally active regions of the genome [9]. R-loops are believed to form naturally from transcription, from double strand breaks, and from defects in mRNA processing/export [9,10]. It is observed that in regions of DNA with an increase in transcription there is also an increase in R-loops, further supporting the idea that they form during transcriptional processes. As RNA Polymerase II (RNAPII) moves along DNA during transcription, a strand of RNA forms behind it. Occasionally, the RNA can hybridize to its complimentary DNA strand, forming the RNA:DNA hybrid structure and displacing the other DNA strand (Figure 1), although, some data suggests that R-loops can also form during polymerase backtracking [1,11]. The longer the nascent RNA strand exists near single-stranded DNA (ssDNA), the higher the likelihood that DNA and RNA will hybridize. This is why double strand breaks, causing RNA Polymerase II stalling, and nascent RNA processing/export defects can cause an increase in R-loops [9,12]. Both issues involve

RNAPII stalling along with a newly formed RNA strand being trapped in between two single strands of DNA (Figure 1). This increased duration of time that the RNA strand spends in the ssDNA environment only acts to increase the likelihood that an R-loop forms. Due to this, there are multiple possible ways to accumulate R-loops and the cells must act quickly to export the pre-mRNA in an efficient manner, or otherwise risk R-loop accumulation.

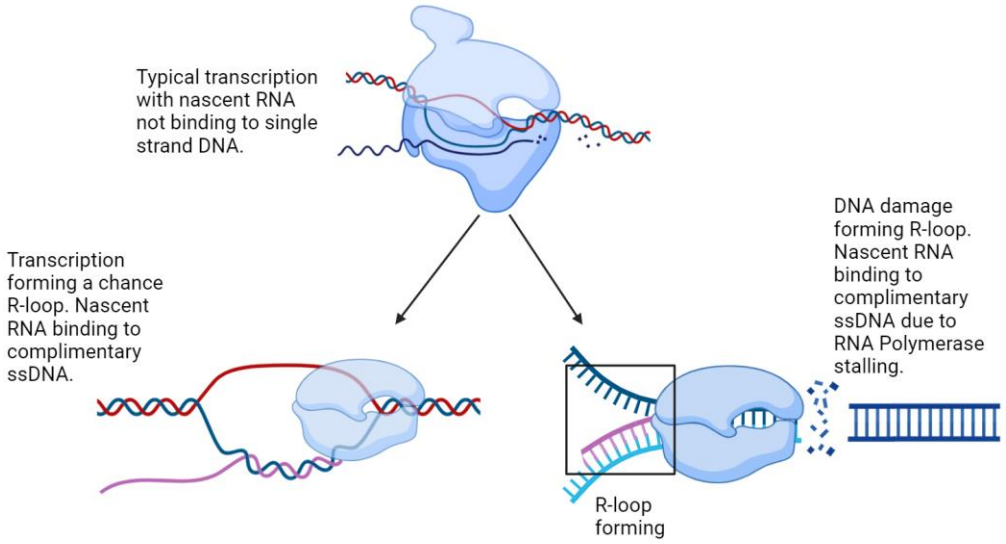

Figure 1: Nascent RNA Binding to Complimentary DNA is the Dominant Mechanism of R-Loop Formation. Bottom left of the image shows R-loops forming by chance from transcription. Bottom right of the image shows RNA polymerase stalling due to a double strand break and forming an R-loop.

Regulatory Role of R-Loops

R-loops form constantly throughout the genome. The cell has a certain number of constant R-loops which has been approximated at 300 R-loops per cell with a half-life of 11 minutes [13]. It is believed that 27,000 R-loops are resolved per day per cell [14], and they occupy approximately 5% of the mammalian genome [15,16]. R-loops are found throughout the genome, including repetitive sections like telomeres, centromeres, and non-coding repetitive regions [17-19].

The extensive existence of R-loops under normal physiological conditions means that not every R-loop is impairing the normal functions of the cell. It is known that if a cell has too few R-loops it will alter the gene expression of a multitude of genes [20], while having too many R-loops causes genomic instability and can lead to cancer or other neurologic disorders [21].

R-loops play an important regulatory role in mitochondrial replication. R-loops residing in mitochondrial DNA could initiate strand asynchronous mitochondrial DNA replication along with determining the replication mechanism of choice in the circular mitochondrial DNA (mtDNA) [22]. R-loops also play an important role in immunoglobulin (Ig) class switching − the region in the Ig genes where recombination or rearrangement occur [23]. There are five different classes of immunoglobulin heavy chains, and switch regions are found on genes encoding every class type [24]. Class switch recombination requires activated-induced cytidine deaminase (AID) inside B cells [25]. AID only deaminates cytosines to uracils when the DNA is single stranded [26]. R-loops are detectable at certain switch regions, and they provide specific target sites for AID recognition [23,27]. Without R-loop formation in these precise locations, the immune system would likely not be as diverse and robust as it is. Another important regulatory function of R-loops is its role in preventing telomere shortening and cell senescence [28]. Npl3 (RNA binding protein that plays a role in RNA biogenesis) binds to the long non-coding RNA transcribed from telomeric repeats (known as TERRA) and preserves R-loops at telomeres [28, 29]. The stabilization of R-loops at short telomeres promotes homology directed repair to extend telomere lengths, which in turn stops premature replicative senescence [28]. R-loops are also thought to prevent c-MYC activation along with regulating CRISPR processes [14,30]. These examples show that R-loops are not all unwelcome and play some vital roles in the success of a cell. Without a tight regulation of

how many R-loops, where they are, and how long they are allowed to persist, the cell would probably not be able to function properly. There are likely more regulatory roles that R-loops play still waiting to be discovered. When one thinks of R-loops it is easy to only wonder about the negative effects they cause in cells, but one should remember they are vital for the success of a cell when properly regulated.

Effects of Abnormal R-Loops Accumulation in Cells

Cells have lots of R-loops and must exist in a homeostatic quantity inside the cell or else chaos can unfold. Abnormal R-loop accumulation can lead to replication stress, double strand breaks, TRCs, transcription pauses, chromosome instability, and gene expression changes [1]. Abnormal R-loop formation stalls DNA polymerases. The stalled replication can cause RNA Polymerases to disrupt fork progression, causing DNA damage, which is a hallmark of genomic instability [31]. The cell can also simply cut out the entire R-loop, leaving a lone ssDNA inside the genome. DSB repair proteins are recruited to the cut site to fix the break. If these repair mechanisms make mistakes, it will lead to increased genome instability [32]. Along with increased genomic instability, an increase in R-loops also changes the protein being made. Many R-loops are found in promoter and enhancer regions and could act as targets for transcription factors to promote gene expression. For example, the anti-sense lncRNA VIM-AS1 (vimentin antisense RNA 1) activates the VIM (vimentin) gene, which then forms an R-loop downstream, promoting NF-kB transcription factor recruitment [18]. In addition, increased R-loops are found to turn off/on the expression of specific DNA repair or R-loop resolution genes that aid in R-loop resolution, further exacerbating the effects of increased R-loop formation [33]. For all these reasons stated, it is

critical the cell be able to respond to increased R-loop formation quickly and accurately. Thankfully, the cell has many tools to fight back against aberrant R-loop accumulation.

Cell Capabilities in Resolving R-Loops

R-loops are more thermodynamically stable than dsDNA. This forces the cell to expend energy in order to enzymatically remove these structures [1]. Cells without the function of resolving R-loops have little to no chance of survival, exhibiting the importance of R-loop resolving proteins. Multiple RNA-DNA helicases such as DDX5 and DDX21, Senataxin (SETX), and RNaseH enzymes, as well as DNA Topoisomerases are found to prevent the accumulation of R-loops [34-38]. Senataxin and RNaseH (RNaseH1 and RNaseH2) enzymes have specialized ability to unwind RNA:DNA hybrids. RNaseH resolves R-loops by binding to the RNA-DNA hybrid region of the R-loop and cleaving the RNA strand. Once the RNA is degraded, the DNA strand can re-anneal to its complementary DNA partner, restoring the normal DNA double helix structure and resolving the R-loop [39]. The RNaseH enzymes have two different forms in eukaryotes, RNase H1 and H2, both of which cleave RNA in R-loops. RNaseH1 works throughout the cell cycle and appears to become activated when R-loop abundance is increased [40]. On the other hand, RNaseH2 has a much stricter cell cycle requirement of when it can be active and is crucial in G2/M phases [40]. RNaseH1 is found in prokaryotes and eukaryotes while RNase H2 is found in all branches of life [41]. Defects in RNaseH2 cause Aicardi-Goutiéres-Syndrome, a damaging neurologic disorder [42]. Due to the serious effects relating to defects in RNaseH, it is important to continue research aiding in further understanding of RNaseH and the differences between RNaseH1 and RNaseH2.

SETX is a helicase that unwinds the RNA:DNA structure of the R-loop. It has a broad range of effects relating to decreasing R-loop abundance and maintaining genome stability. Its malfunction has been linked to notable neurologic disorders such as ALS4 (Amyotrophic Lateral Sclerosis Type 4) and AOA2 (Ataxia-Ocular Apraxia Type 2) [20]. In addition to resolving RNA:DNA hybrids, it also plays a role in RNAPII transcription termination, regulating gene expression, and regulating TRCs [34, 20]. SETX is believed to be associated with the transcription machinery. This association suggests that it may play a role in preventing R-loop formation during active transcription or in promptly resolving them should they form. Overall, the specific action of how SETX resolves R-loops is poorly understood, and the change in R-loop abundance upon SETX impairment could be due to the change in gene expression or aiding in transcription termination [34].

Aside from the previously mentioned R-loop resolving enzymes, numerous proteins have been found to modulate R-loop abundance. These proteins can bind to, stabilize, resolve or degrade RNA:DNA hybrids, thereby orchestrating R-loop homeostasis. R-loopBase, a recently launched database, offers an exhaustive and current catalog of these R-loop regulators [43]. As of now, nearly 1,200 proteins are recognized as either established or potential R-loop regulators in human cells [43]. However, the specific regulatory mechanisms underlying the vast majority of these proteins remain to be elusive [43]. These proteins are integral to diverse cellular processes, spanning DNA repair, replication, RNA processing, DNA topology, epigenetics, chromatin structure, transcription, non-coding RNAs, cell cycle management, and cellular stress responses[43]. The vast array of R-loop regulators underscores the pivotal role of R-loop homeostasis in maintaining normal cellular activities and ensuring genomic integrity.

Effects of R-Loop Formation on Gene Expression

Either the reduction of R-loop formation or overaccumulation of R-loops can cause drastic effects in gene expression. In previously mentioned neurologic disorders AOA2 and ALS4, there is a significant change in SETX function [20]. In AOA2, SETX function is reduced, causing a major accumulation of R-loops, whereas in ALS4 the ability of SETX to resolve R-loops is enhanced, resulting in less R-loops [20]. In ALS4 patients, R-loop decrease occurs primarily in the TSS (transcription start site) and CPS (cleavage and polyadenylation site) regions of genes [20]. Due to the lack of R-loops, TSS region is over-methylated, reducing mRNA levels of genes such as BAMBI, which helps regulate the TGF-β pathway [20]. Similar results have been observed in the mTOR pathway [44]. As R-loop abundance decreases, mTOR is downregulated, further supporting that a lack of R-loops decreases gene expression [44]. mTOR controls embryonic stem cell commitment to trigger diapause [45] and is crucial in developing embryos among many other cellular processes. Researchers have demonstrated that the activity of DNA methyltransferase 1 (DNMT1) on dsDNA is 2.5-fold higher than on RNA:DNA hybrids, suggesting that DNMT1 is repelled by R-loops [45]. DNMT1 functions by transferring a methyl group onto the C5 position of cytosine [46]. The addition of a methyl group decreases gene transcription by inhibiting transcription factors from binding or recruiting gene repression proteins [46]. When testing for R-loop vs methylation throughout the genome, researchers were able to determine that R-loops regulate methylation of more than 1,200 human genes [20]. This result shows that R-loops play a crucial role in gene expression, providing another example of why R-loop levels exist in a homeostatic amount. The cell must tightly regulate when an R-loop is beneficial and when it is time to resolve R-loops. The epigenetic effects of R-loop on gene

silencing should not be underestimated either, with further research needed to determine the exact effects of R-loops on epigenetics. How the cell knows when to resolve an R-loop to permit methylation is an important and yet poorly understood question in which more research is needed.

Detecting R-Loops and the Controversy Behind it

The current options for detecting the location and quantity of R-loops are limited. One approach utilizes the S9.6 antibody, which binds to RNA:DNA hybrids (Figure 2). To map the location of R-loops in the genome, DRIP-seq (DNA-RNA immunoprecipitation using the S9.6 antibody and then coupled with high throughput DNA sequencing) has been developed [47]. The problem with the S9.6 antibody is that it non-specifically binds dsRNA, introducing potential errors in results [48, 49,50]. An alternative technique employs a catalytically inactive RNaseH1 variant (D210N), which binds to the RNA in the RNA:DNA hybrid without resolving the R-loop [51]. This variant is also used in a procedure known as R-ChIP, where R-loops are captured by chromatin immunoprecipitation using an antibody to pulldown D210N [52]. Notably, studies indicate discrepancies between the results from the DRIP and the R-ChIP methods. Both RNase H1 and S9.6 seem to detect dsRNA at levels only 20 times lower than RNA:DNA hybrids [48]. This quandary regarding the two detection methods presents major obstacles in obtaining reliable, accurate, and reproducible data regarding R-loop formation in the genome. Another advanced method, SMRF-seq, uses non-denaturing bisulfite R-loop footprinting coupled with high-throughput single molecule sequencing. It works by promoting the deamination of single-stranded cytosines in the unbound strand of an R-loop, converting them to uracils [53, 54]. Because SMRF-seq targets three-stranded structures, it offers high specificity. It can also achieve near

single-nucleotide resolution in NTERA-2 cells [53, 55]. However, this technique has its drawbacks. It can't detect R-loops in highly methylated C and poly(A) tracts [56, 55] and may overestimate R-loop numbers if there's ssDNA present in the cytosol or nucleus. Furthermore, it assumes stable, non-helical DNA in eukaryotes, which isn't always the case, potentially leading to underestimation [57,58, 59]. Overall, each R-loop detection method comes with its own advantages and limitations. There isn't a universally superior method. For the most reliable results, researchers should consider employing multiple methods to cross-verify findings and account for potential discrepancies.

R-Loops, Cancer, and the Therapeutic Possibilities

One cancer in which R-loops are prevalent is Ewing Sarcoma, a cancer of the bone and soft tissue caused by a chromosomal translocation, most commonly t(11;22)(q24;q12), which results in a fusion gene known as EWS-FLI1 [60,61]. Ewing Sarcoma tumors show an increased R-loop abundance when compared to other sarcoma tumors [60]. In cancers with the mutated BRCA1, a decrease in function of BRCA1 has been found to cause an increase in global R-loops, inducing genomic instability, altering transcription and epithelial differentiation [62]. Having a deficiency in BRCA1/SETX activity causes unrepaired ssDNA breaks on the non-bound strand of DNA at R-loop termination regions [63]. Abnormal R-loop formation may also drive acute myeloid leukemia (AML). Data have indicated that R-loop formation is vital in maintaining HOXA gene family topologically associated domain integrity, which promotes β-catenin and its target gene expression, increasing AML leukemogenesis [64]. The recent data on the prominent roles of R-loops in multiple different types of cancer suggests its power over the genome is quite large. This cancer data, combined with previously known data concerning R-loop’s ability to

effect transcription, genome instability, and DNA damage, indicate that it may be helpful to examine R-loop abundance and location in all types of cancer [65, 66].

Due to R-loops ability to induce genomic instability and replication errors, there is a growing interest in deliberately promoting R-loop accumulation in cancer cells, with the rationale that excessive R-loop formation may compromise cell function, ultimately leading to cell death [67]. Efforts are underway to exploit this vulnerability by intentionally augmenting R-loop levels in cancer cells. One notable gene is BRD4, when silenced causes an increase in R-loops [10]. BRD4 regulates gene transcription by recruiting transcription proteins to acetylated histone residues [68,69]. Previous research has inhibited BRD4, suppressing cell proliferation, and inducing apoptosis in various cancers including AML [70], large B cell lymphoma [71], and breast cancer [72]. While the exact mechanism underlying the anti-proliferative effect of BRD4 inhibition is multifaceted, a significant contributing factor appears to be the increase of R-loops. It has been found that BRD4 inhibition leads to a reduction in ATR/CHK1, a cell cycle checkpoint regulator, causing cells with extensive impairments to prematurely enter mitosis [10]. Furthermore, it reduces the transcription of genes involved in homologous recombination. Additionally, BRD4 loss increases R-loop-induced DNA damage throughout the genome, especially in genes that typically resolve R-loops, thereby further increases the amount of R-loops [10]. This finding about BRD4 highlights the potential therapeutic impact of modulating R-loop abundance. Harnessing this approach might provide a promising avenue in cancer therapy and holds potential across a diverse range of cancer types.

Senataxin

Senataxin (SETX) is a helicase that unwinds the RNA: DNA portion of the R-loop[73]. It has

a broad range of effects relating to decreasing R-loop abundance and maintaining genome stability. Its malfunction has been linked to notable neurologic disorders such as ALS4 (Amyotrophic Lateral Sclerosis Type 4) and AOA2 (Ataxia-Ocular Apraxia Type 2)[20]. In addition to resolving RNA:DNA hybrids, it also plays a role in RNAPII transcription termination, regulating gene expression, and regulating TRCs (transcription replication collisions) [20,73]. SETX is believed to be associated with transcription machinery. It is known that SETX interacts with polyadenylation binding factors and RNA Polymerase II [74]. This association suggests that it may play a role in preventing R-loop formation during active transcription, or in promptly resolving them should they form. The interaction with transcription machinery and R-loops further enhances the likelihood that SETX affects gene transcription in a variety of ways. Research has shown that decreasing abundance of SETX inside the cell leads to an increase in R-loops in mice and humans furthering proving its role in R-loop resolution, and a promising gene to target in attempts to increase genomic R-loop abundance [75].

Nucleolus and Nucleolar Stress:

The nucleolus is the location in the nucleus where rDNA transcription, rRNA modification, and assembly of ribosomes occur. This is the most energetically intensive process in the cell [4,5]. Nucleoli have three distinct compartments. The fibrillar center (FC), the dense fibrillar component (DFC), and the granular component (GC) [76]. The FC is where transcription of rDNA occurs by RNA Polymerase I, the DFC is where rRNA processing proteins such as fibrillarin occupy, and the GC is the compartment in which rRNA processing and ribosome subunit assembly occurs along with other ribosomal proteins and nucleolar organizers such as NPM1[76]. Typically, healthy nucleoli have an irregular shape with the GC found throughout the nucleolus

and the fibrillarin components exist separately, but inside, the GC of nucleoli[76]. In cancer cells, nucleoli are typically increased in size and/or number due to the increased protein production a cancer cell needs to survive, a sign of poor prognosis in many cancer types [6,7].

Nucleolar stress is a loose term relating to a change in morphology or function of the nucleolus [76]. Currently, known nucleolar stressors include anticancer agents, UV, hypoxia, heat shock, nucleotide depletion, and oxidative stress [77,78]. Previous data has indicated that under conditions of hypoxia nucleolar R-loops increase and global transcription decreases[79]. Following nucleolar stress, nucleoli become spherical with NPM1 (GC) forming a spherical ring and fibrillarin (FC and DFC) concentrating in locations along the sphere [76]. During the morphology change of nucleoli under conditions of stress; RPL5 (ribosomal protein L5), RPL11, and 5S rRNA are distributed differently inside the nucleoplasm. These proteins and rRNA then interact with MDM2 and MDM4 (HDM2 in humans), ubiquitin ligases for p53, and block MDM2 and MDM4 from interacting with p53 [78,80]. Other findings indicate that HDM2-p53 interaction is inhibited due to NPM1 translocation to the nucleoplasm and binding to HDM2 which allows for an increase in nucleolar p53 levels [78]. Despite the exact mechanism being unclear, nucleolar stress causes p53 levels to increase. This allows p53 to recognize the nucleolar stress inside the cell and perform cell cycle arrest or apoptosis of that cell [81].

NPM1

NPM1is a protein that is concentrated in the nucleolus and is vital to the success of ribosome biogenesis and assembly. Inside the nucleolus, NPM1 exists in the granular component of the three-phase condensate. Overall, it plays a role in mRNA processing, chromatin

remodeling, and genomic stability along with its previously mentioned role [82]. NPM1 is considered a good sensor of any cellular stress. Specifically, under conditions of nucleolar stress NPM1 will be translocated from the nucleolus into the nucleoplasm [78]. When cells undergo drug treatments that stop rRNA transcription and early processing, NPM1 will translocate to the nucleoplasm [83]. Once the translocation of NPM1 to the nucleoplasm occurs, due to nucleolar stress, the protein will bind to and sequester MDM2 making the ubiquitin ligase unable to perform its function [82]. This activity of sequestering MDM2 allows for an increase in the amount of p53 inside the cell. For these reasons, the location of concentrated NPM1 is a very useful strategy in determining when a cell is undergoing nucleolar stress, and accounts for the increased levels of p53 seen under nucleolar stress. However, other proteins such as RPL11 or RPL5 also can bind and sequester MDM2 regardless of NPM1[84]. Due to this NPM1 should be seen as one of many possible indicators that a cell is undergoing nucleolar stress, but it is a good indicator, nonetheless.

p53

A tumor suppressor protein is a protein that, once activated, acts to decrease the cells' ability to further proliferate. p53 itself promotes cell arrest or apoptosis in cells once activated. However, p53 is an activator of proteins that specifically cause apoptosis or cell cycle arrest. Once activated, p53 increases the transcription of another tumor suppressor protein p21 or Bax [78]. Bax induces apoptosis in cells while p21 promotes cell cycle arrest to allow the cell time to fix whatever issues it is having [78]. Levels of p53 are typically kept lower in a cell due to the ubiquitination of p53 by ubiquitin proteins. An important E3 ubiquitin ligase for this thesis is HDM2. HDM2 is the human form of MDM2 which ubiquitinates p53, signaling it for

degradation and keeping levels of p53 low. However, as previously mentioned, under nucleolar stress sequestering of MDM2 by proteins such as NPM1 causes the stability of p53, leading to higher levels of p53 and an activation of cell arrest or apoptosis. In studies with reduced binding of p53 to MDM2; levels of p53 are increased similar to how p53 levels are increased under conditions of nucleolar stress [85].

Fibrillarin

Another protein vital in ribosome biogenesis is the protein fibrillarin which is heavily concentrated in the nucleolus. Fibrillarin has been highly conserved evolutionarily, showcasing its importance in the overall success of cells [86]. Fibrillarin is concentrated in two compartments of the nucleolus, the FC and the DFC. Fibrillarin is a methyltransferase capable of modifying and degrading rRNA [87]. It can methylate over 100 different sites and is vital for pre-ribosomal processing along with aiding in ribosome stability [88]. Fibrillarin is an abundant nucleolar protein whose location changes under nucleolar stress. When cells are unstressed, fibrillarin generally appears spread out and in odd shapes found throughout the nucleus and in larger amounts in the nucleolus. Under nucleolar stress, the protein will aggregate to the edges of the nucleolus and prominent concentrated fibrillarin “caps” can be seen [76]. Under immunofluorescence staining, fibrillarin can be highly useful in visualizing when the cell is undergoing nucleolar stress due to the fibrillarin “caps” in the shape of a donut.

Actinomycin D.

The primary RNA polymerase involved in ribosome biogenesis is RNA Polymerase I (RNA Pol I). A consistently reliable way of causing nucleolar stress in cells is impairing the activity of Pol I. Actinomycin D (Act. D) induces its’ effects on the cell by binding to G/C rich

regions of DNA [89]. At high concentrations (>800nM) Actinomycin D acts a very potent polymerase inhibitor leading to high levels of toxicity in cells [90]. It has many anti-tumor capabilities, but Act. D. is not useful in studying nucleolar stress at such high concentrations due to its effects on all polymerases leading to cell death. At concentrations between 2 nM and 100 nM, Act. D. specifically targets RNA Polymerase I [90]. This is likely due to the high levels of G/C content in ribosomal DNA causing low concentrations of Act. D. to preferentially intercalate at regions of DNA transcribed by RNA Pol I. Due to this, low doses of Act. D. will cause nucleolar stress in the cell by inhibiting the function of RNA Pol I. This makes Act. D. a very useful tool, as a control, to elicit nucleolar stress in cells while allowing other functions of the cell to remain as unperturbed as possible.

Rationale of the Research

There is a lack of research regarding whether aberrant R-loops alone can increase nucleolar stress. However, it is known that cellular levels of tumor suppressor p53 increase after nucleolar stress in comparison to non-stressed cells [8]. Understanding if aberrant R-loops alone elicits nucleolar stress will expose a new method for causing nucleolar stress. It is important to test if this increase in nucleolar stress correlates with a decrease in cell viability due to the increased p53 levels caused by nucleolar stress. This will allow R-loops to be targeted in cancer cells to induce cell death through the nucleolar stress pathway, which was previously unknown. Testing this will involve tracking R-loop abundance and localization (tested by dot blot, IF, and live-cell imaging) under differing conditions of stress such as DNA damage inducing and repair inhibiting agents, determining if a possible increase in R-loops can cause nucleolar stress (tested by IF) and p53 accumulation in cells (tested by western blot), and if this p53 activation causes

increased cell death or growth arrest (tested by counting cells after treatment). I hypothesize that increasing R-loops will cause an increase in nucleolar stress, activating p53, and resulting in increased cell death.

This manuscript aims to understand a possible new way to attack cancer cells. To understand the manuscript, one must understand the research is very limited in literature. The idea behind the research done in this manuscript was inspired by the background. Recently, the studying of R-loops has become more prevalent. This has allowed more understanding in the scientific community. From new literature regarding nucleolar stress and R-loops, it appears that these two processes have a wide array of causes; some of which are the same. This increased understanding has allowed new predictions/hypothesis to be made from previous data. The new prediction for this manuscript was that two phenomena inside cells could be linked. If the connection between R-loop and nucleolar stress is confirmed, this link could present a novel method to attack cancer cells. However, proving the link between these two very common phenomena inside cells is a difficult task to undertake and will require many different approaches to confirm.

CHAPTER TWO

MATERIALS AND METHODS

Cell Culture

All cells were cultured in 10% calf serum (CS)/Dulbecco's Modified Eagle Medium (DMEM). Cells were incubated at 37°C in 5% CO_2. U2OS and HBD-EGFP U2OS cells used.

Live-Cell Imaging to Visualize the Localization of Nuclear R-loops Upon Drug Treatment

Osteosarcoma cell line U2OS stably expressing doxycycline-inducible HBD-EGFP were used in live cell imaging. This cell line was created in the Chai lab prior to me joining the lab (unpublished). Basically, the catalytically inactive RNase H1 (the hybrid-binding domain, HBD) and the nuclear-localization signal (NLS) are fused to EGFP, and cloned into the pLVX-Puro lentiviral vector that contains a tet-on doxycycline inducible promoter. Upon addition of doxycycline, HBD-EGFP is expressed and binds to, but does not resolve, nuclear R-loops. This method allows for direct visualization of nuclear R-loops in live cells.

Cells were seeded in 6-well dishes and allowed to attach overnight. Post seeding all wells were given 100 ng/mL of doxycycline. Then, one well was given 1 μM of Olaparib overnight and another was given 2.5 μM overnight. The next day other chemotherapeutic agents were added to the remaining wells before imaging. CPT was added for one hour to a final concentration of 1 μM, MMC was added for one hour to a final concentration of 10 μM, MMS was added for one hour to a final concentration of 1μM, Cisplatin was added for one hour to a

concentration of 50 μM, Camptothecin (CPT) was added for one hour to a concentration of 1 μM, along with a control well that only received doxycycline. Cells were imaged on a Nikon Eclipse Ti2 inverted fluorescent microscope at 40x.

Quantification of Live-Cell Imaging

Quantification of live cell imaging was done by counting R-loop "zones" manually and then averaging the number of zones per cell for each treatment. R-loop zones were green concentrated dots seen in each cell. The green dot was the visualization of the catalytically inactive RNase H1 bound to R-loops, thus allowing visualization of R-loops. Quantification was also confirmed by IMARIS 8.0.2 software (Oxford Instruments) measuring individual fluorescence points bigger than 3μm in diameter after activation of the catalytically inactive RNase H1.

siRNA Transfection of SETX

U2OS and HBD-EGFP U2OS cell lines were used for transfection. Cells were seeded at 70-85% confluency in a 6-well plate and allowed to attach overnight. The next day a master mix was made of 300 μL of OPTI-MEM and 18 μL of RNAiMAX (Invitrogen). A control Eppendorf tube was made with 150 μL of OPTI-MEM and 2 μL of 20 μM siControl (Dharmacon, targeting sequence- uuc ucc gaa cgu guc acg u). Next, a Senataxin Eppendorf tube was made with 150 μL of OPTI-MEM and 2 μL of 20 μM siSETX (Dharmacon, targeting sequence- gag aga auu auu gcg uac u). 150 μL of the master mix tube was added into the control tube. This was repeated for the SETX tube. Both tubes, now containing 300 μL of solution, incubated for 5 minutes at room temperature to allow mixing. The siControl tube was then added dropwise to one well. Then, the siSETX tube was added dropwise into a different well. Lastly, one well was left untouched from

any siRNA. The transfection was given 48-72 hours to proceed before cells were removed from their wells.

Western Blotting

Cells were collected in a pellet and re-suspended in 1% CHAPS buffer (Nuclease free water mixed with OmniPur CHAPS powder to a final concentration of 1%) on ice for 30 minutes before being spun down at 4°C at 21,100 rpm for 15 minutes. A portion of lysate was taken out and mixed with an equal volume of 2X SDS loading buffer/0.2M DTT. This solution was then heated at 95°C for 5 minutes. After, the lysate mixture was loaded onto an SDS-PAGE gel. A 10% gel was made for actin, GAPDH, or p53 while a 6% gel was made for Senataxin. The gels were run at either 120V for 90 minutes or 150V for one hour in running buffer. The gels were then transferred to the transfer apparatus (Invitrogen PowerEase Touch 350W) and run at 20V for 90 minutes in transfer buffer. After transfer, the membranes were blocked for one hour on a room temperature shaker in 5% non-fat milk/ 1x phosphate-buffered saline with Tween 20 (PBST). Then, primary antibodies were diluted in 1x PBST and placed in a pouch overnight. Anti-SETX (Bethyl, A301-104A-T) antibodies were diluted 1:2,000, while anti-Actin (Millipore, MAB1501) antibodies were used at a final concentration of 1:60,000, anti-GAPDH was used at a final concentration of 1:60,000 (Proteintech, HRP-60004), and anti-p53 was used at a final concentration of 1:500 (BD Biosciences, 554169). The next day both membranes were washed four times for five minutes each in 1x PBST. Secondary antibodies were added to each membrane in 5% non-fat milk/PBST and placed on a tilter for one hour at room temperature. HRP goat anti-rabbit (Vector Laboratories, PI-1000) for the SETX membrane is diluted 1:10,000. HRP horse-anti mouse (Vector Laboratories, BA-2000-1.5) was diluted 1:5,000. After

secondary antibody had finished the membranes were washed three times for five minutes eachin 1x PBST before applying chemiluminescence solution (ThermoFisher, Super Signal West Femto) at 1:5 concentration, and imaging on an iBright imager.

Immunofluorescence

Cells grown on chamber slides were fixed with 4% PFA in 1x PBS for 10 minutes at r.t. Then cells were washed three times in 1x PBS aspirating out the PBS immediately. After fixation, cells were permeabilized on a shaker for 15 minutes. Cells were then washed three times in 1x PBS for five minutes each. After this, cells were blocked in 10% BSA/1x PBS for one hour in a humidified container at 37°C for one hour. Next, cells were given two primary antibodies. The first primary antibody was given at concentrations of 1:1,000 or 1:500 of anti-Fibrillarin (ThermoFisher, MA3-16771) in 1x PBS. The second antibody was given at concentrations of 1:100 or 1:200 of anti-NPM1 (ThermoFisher, PA1-029) in 1x PBS. After incubated at 37°C for one hour in a humidified container, cells were washed three times in 1x PBS for five minutes each. Then, anti-IgG conjugated to goat anti-mouse Alexa fluor-488 (Invitrogen, A11029, 1:250) and anti-IgG conjugated to goat anti-rabbit Alexa fluor-649 (Thermo Scientific, KB1311197, 1:500) antibody mixtures were made. Both secondary antibodies were diluted in 1x PBS. Cells were then placed in dark on a room temperature shaker for one hour. After, cells were washed in 1x PBS three times, once for five minutes, once for three minutes, and once immediately removed, all washes in the dark. The chamber slide then went through an ethanol series (70% ethanol for one minute, 85% ethanol for one minute, and 100% ethanol for one minute) in the dark. The chamber slide was allowed to air dry until ethanol had evaporated. 10-15 μL of mounting medium containing DAPI (VectorLabs) is added to a

cover slip. The cover slip was placed over the chamber slide and clear nail polish was addedaround the edges of the cover slip. Chamber slide was then stored in a -20°C freezer until imaging.

DNA Extraction and Quantification

Genomic DNA was extracted with PureLink Genomic DNA Mini Kit (Invitrogen) without RNase A. Isolated genomic DNA was collected in autoclaved milliQ water instead of elution buffer. Quantification was obtained using NanoDrop 2000.

Dot Blot

Eppendorf tubes were filled with 15 μL of autoclaved milliQ water containing 750 ng of DNA. Two tubes per treatment. One tube was given 2.5U of RNase H1 (NEB, M0297S or M0523S) and RNase H buffer with the tube containing a final volume of 17 μL. RNase H1 was given as a control for nonspecific binding of the S9.6 antibody. The S9.6 antibody recognizes RNA:DNA antibodies with a high affinity and allows for visualization for relative R-loop abundance in genomic fragments. The other tube was given 2 μL of RNase H buffer (NEB M0297S or M0523S). Tubes were then placed in a 37°C water bath for 20-25 minutes. From each tube, a 2 μL drop of the solution was added onto a nitro cellulose membrane a total of six times (12 μL total). This was repeated for the other tube, directly under the prior six drops. Then, the genomic content was crosslinked to the membrane with UV light (Stratagene UV Stratlinker 1800). After this, cells were blocked in 5% non-fat milk/ 1x PBST for one hour on a rocker. Next, the membrane was split in half (so there are now three “drops” per treatment/tube on each membrane). One half of the membrane was given an anti-dsDNA (Abcam, ab27156) primary

antibody in 5% milk/ 1x PBST at 1:5,000 concentration. The other half of the membrane was given an anti-S9.6 (Sigma, MABE1095) primary antibody in 5% milk/ 1x PBST at 1:5,000 concentration or 1:2,000 concentration. Both membranes were then placed on a rocker at 4 degrees overnight. Next, the membranes were washed three times for five minutes each in1x PBST. After this, a HRP horse-anti mouse secondary antibody was added to both membranes at 1:8,000 for one hour on a room temp tilter. Cells were then imaged using a 1:5 concentration of SuperSignal West Femto solution.

Dot Blot Quantification

Images were taken on an iBright imager and the fluorescence in each dot was calculated for using iBright ™ analysis software. Relative abundance of R-loops was calculated for each treatment by subtracting the RNase H1-treated samples from the RNase H1-untreated samples to remove nonspecific binding of the S9.6 antibody from the relative R-loop count and allow for a more accurate relative fluorescence quantification. Relative fluorescence quantification allowed for a more accurate quantification of the relative number of R-loops in each treatment.

Cell Viability Measurements

Cells transfected following the "siRNA Transfection of Senataxin protocol" were then given 2.5 μM Olaparib overnight, 50 μM Cisplatin for 1 hour, or no chemotherapeutic agent. After the chemotherapeutic agent treatments had finished cells were trypsinized and stained in equal parts trypan blue and cell mixture before counting cells at 10x using a hematocytometer. Cells were counted in 4 chambers of a hematocytometer twice for each treatment.

Statistical Analysis

Statistical analysis done using GraphPad Prism.

CHAPTER THREE: RESULTS

I. DETERMINE WHETHER DNA DAMAGING OR DNA REPAIR INHIBITING CHEMOTHERAPEUTIC AGENTS AFFECT R-LOOP ABUNDANCE AND LOCALIZATION IN THE NUCLEUS

I hypothesize that DNA damaging or DNA repair inhibiting chemotherapeutic agents will change R-loop formation, either the abundance or the localization or both. To test this, I used two approaches to (1) measure the R-loop abundance and (2) monitor the localization of R-loops inside cancer cells after addition of chemotherapeutic agents that cause DNA damage or inhibit DNA repair. Table 1 lists the chemotherapeutic agents used in this study and their methods of action.

Table 1: List of DNA Damaging or DNA Repair Inhibiting Drugs Used

Drug	MOA	Effect on the cell
Olaparib	Inhibits poly ADP-ribose polymerase	Block the repair of single-strand DNA breaks
Cisplatin	Covalent binding of platinum to purine bases causing cross-linking of bases	DNA damage and DNA replication impairment
Camptothecin (CPT)	Affects topoisomerase I, allowing DNA cleavage, but inhibiting subsequent ligation	DNA damage
Mitomycin C (MMC)	Alkylating agent that inhibits DNA synthesis by cross-linking complementary DNA strands	DNA damage, translation stalling, and can inhibit DNA replication
Methyl methanesulfonate (MMS)	Alkylating agent that acts on DNA by preferentially methylating guanine and adenine bases	DNA damage and replication issues

1. Determine the effect of DNA damaging or DNA repair inhibiting chemotherapeutic agents on R-loop abundance using a dot blot.

To measure the relative R-loop abundance, the dot blot method was used [91] (Figure 2). Briefly, total genomic DNA was isolated from cells after drug treatments. An equal amount of DNA was split in half, treated with or without RNase H1, and dotted on two membranes. Each sample was dotted in triplicate to get a better overall representation of genomic material contained in each sample. One membrane was probed with the S9.6 antibody, which binds specifically to RNA:DNA hybrids [91]. The second membrane was probed with the antibody recognizing double stranded DNA (dsDNA), which acts as a loading control for overall genomic material dotted onto each membrane. RNase H1 treated samples acted as a control to exclude signals caused by any non-specific recognition of the S9.6 antibody. The results in Figure 3 suggested that R-loop abundance did change after chemotherapeutic addition. Figure 3 suggests that the tested chemotherapeutic agents caused a relative increase in R-loop abundance.

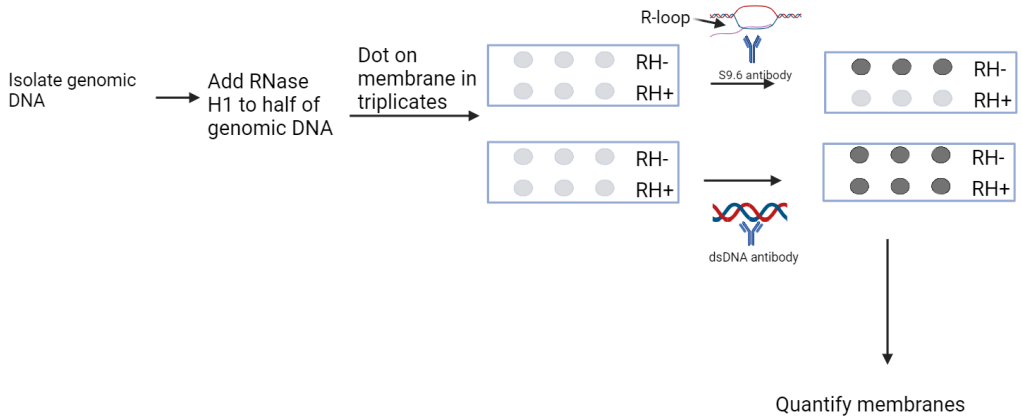

Figure 2: Scheme of Dot Blot to Identify Relative R-Loop Abundance. Figure shows when RNase H1 is added to cells and how membranes dots are ordered before antibody is added. The dots given RNase H1 were labeled "RH+" and dots without RNase H1 were labeled "RH-"

3a

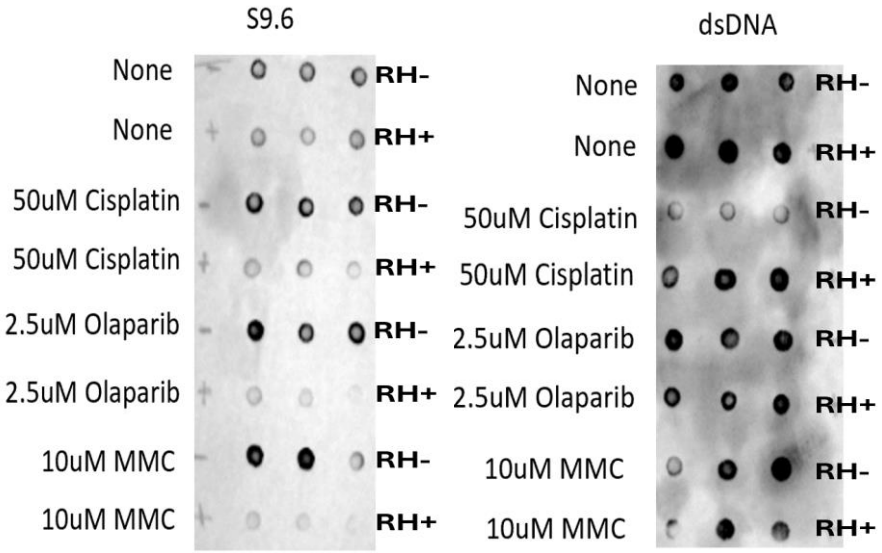

3b

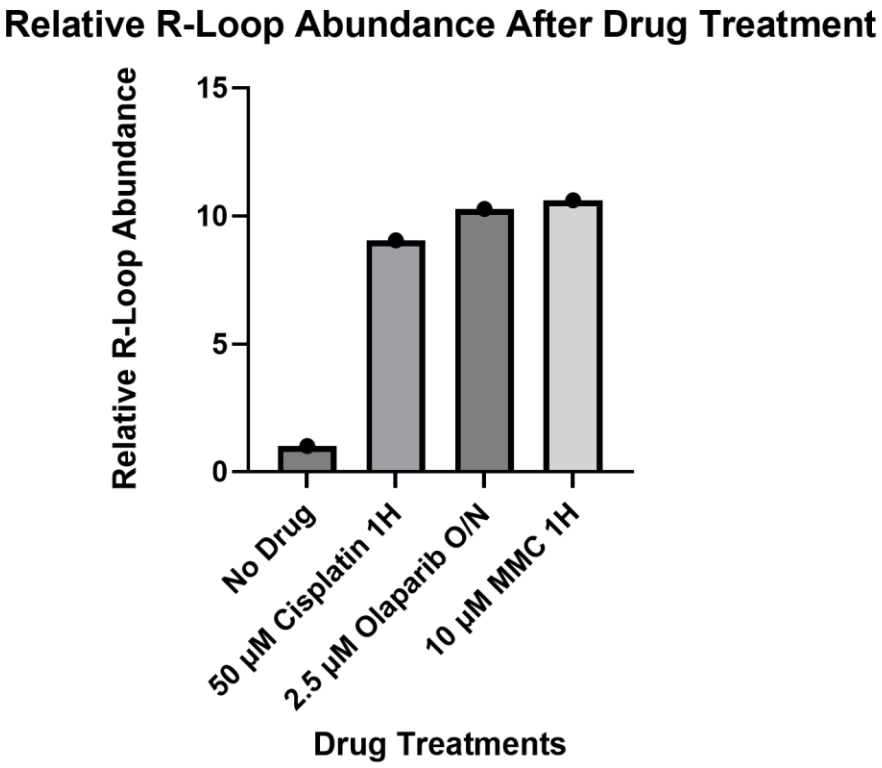

Figure 3: DNA Damaging and DNA Repair Inhibiting Agents Appear to Increase R-Loops. (a) Image of the dot blot membrane after drug treatment, S9.6 antibody, and RNase H (RH+) Addition. Image shows dot intensity of dsDNA and S9.6 antibodies on the membrane. (b) Graph of Quantified Relative R-Loop Abundance. Done by subtracting the RH+ channels from the RH- channels of the same treatment. Fluorescence intensity normalized to no drug treatment data. Dot blot indicates the drug treatmetns chosen likely increase R-loop abundance in cells. However, results were from one experiment, therefore no statistical significance could be determined.

Figure 3 indicates, with the dot blot method, that R-loop abundance increases after a 2.5 µM Olaparib 16-hour treatment, 50 µM Cisplatin 1 hour treatment, and 10 µM MMC 1 hour treatment. This can be seen due to the higher S9.6 intensity (binding of S9.6 antibody which identifies R-loops) when compared to dsDNA (overall genomic abundance in each dot) dot intensity in each treatment type. These results seem to show that DNA damage inducing and

DNA repair inhibiting chemotherapeutic agents likely increase nuclear R-loop abundance.

2. Determine the effect of DNA damaging or DNA repair inhibiting chemotherapeutic agents on R-loop localization using live-cell imaging and a catalytically inactive RNase H1 variant.

To determine whether the chemotherapeutic drugs alter the localization of R-loops in the nucleus, a catalytically inactive RNase H1 variant (HBD) fused to EGFP was stably expressed in the osteosarcoma cancer cell line U2OS (Figure 4). HBD is the RNA:DNA hybrid binding domain of RNase H1 and lacks the catalytic domain. Nuclear-localization signal (NLS) was added to HBD so that HBD only recognizes nuclear R-loops. In addition, the expression of HBD-EGFP is under the control of doxycycline. Upon addition of doxycycline, HBD is transcribed to bind to, but not resolve, nuclear R-loops (Figure 4).

4a

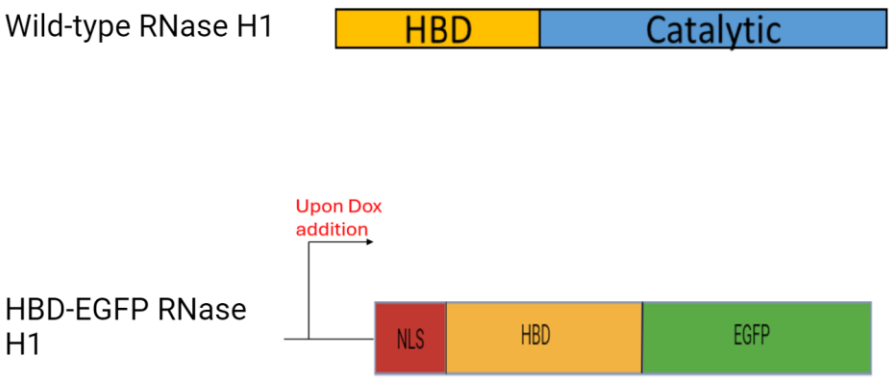

4b

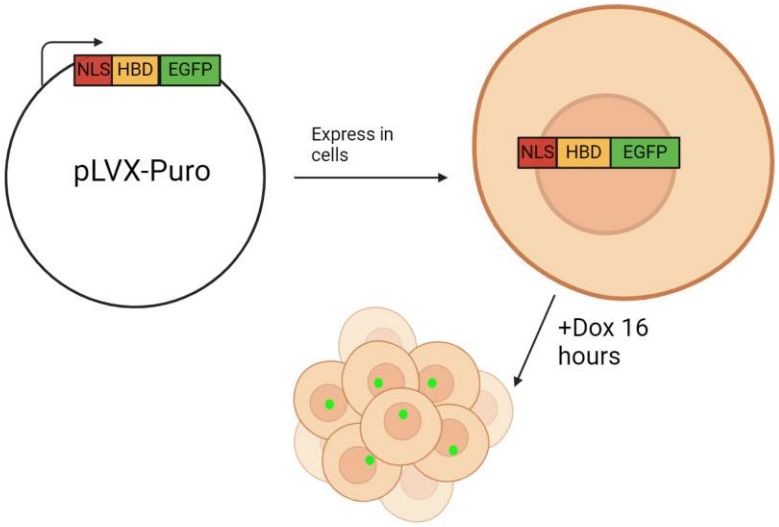

Figure 4: Scheme of Major Domains of RNase H1 and its Catalytically Inactive Variant. (a) Comparing protein domains of WT RNase H1 and HBD-EGFP RNase H1. (b) The RNase H1 hybrid-binding domain (HBD) and the nuclear-localization signal (NLS) are fused to EGFP, and cloned into the pLVX-Puro lentiviral vector that contains a tet-on inducible promoter. Cells stably expressing the doxycycline-inducible HBD-EGFP were made by lentiviral transduction. Cells were then given doxycycline to activate the promoter to transcribe the catalytically inactive RNase H1, then 16 hours later cells fluoresce where the catalytically inactive RNase H1 had bound to R-loops.

Live-cell imaging showed that HBD-EGFP signals were clustered in nuclei, forming large green fluorescent dots (Figure 5a), which we termed “R-loop zones”. Drug treatments did not affect the appearance of R-loop zones. They consistently clustered in large green, fluorescent dots as seen in Figure 5a. To determine whether drug treatments altered the number of R-loop zones, I counted R-loop zones both manually and using the Imaris imaging analysis software. In manual counting, the number of R-loop zones per cell was manually counted, then the total number of zones was divided by total cells counted to find the average number of zones per cell after treatment (Figure 5b). I also used the Imaris 8.0.2 software to count the number of fluorescent dots with a diameter bigger than 3 μm inside the nucleus. The R-loop zone count was kept consistent by choosing a fluorescent size that removed most background but recognized cellular R-loop zones. The drugs treatments were repeated three times and the number of R-loop zones in each HBD-EGFP-U2OS cell was plotted (Figure 6a). The overall average R-loop zones per cell was plotted in Figure 6b to allow an easier comparison to the manually counted method in Figure 5b.

5a

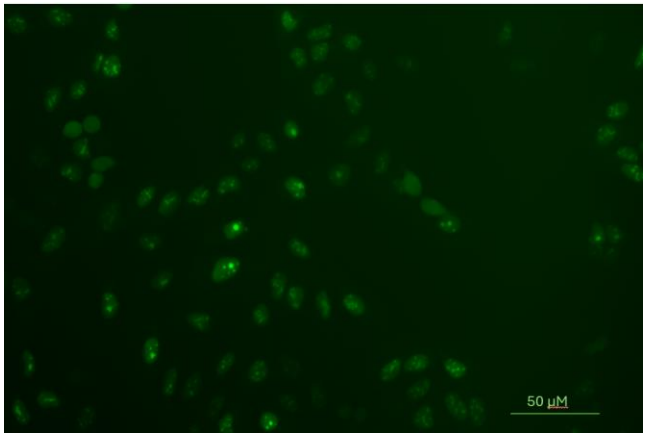

5b

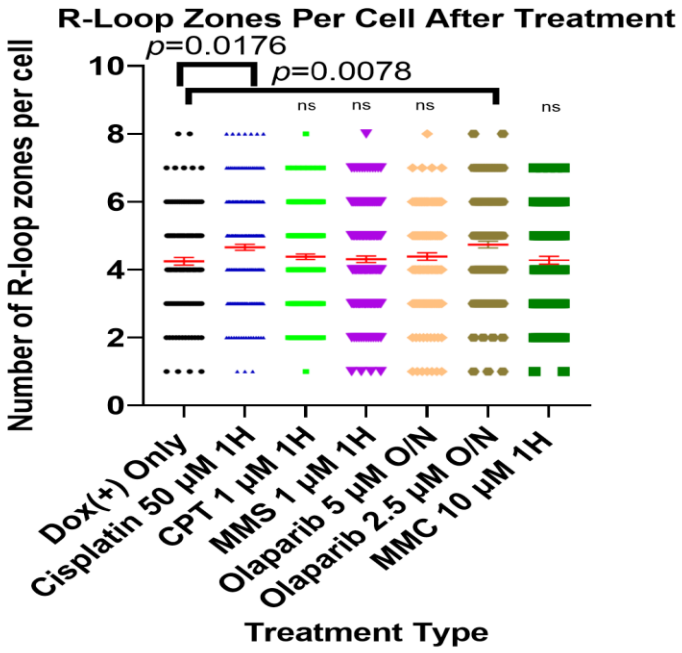

Figure 5: Effect of DNA Damaging and DNA Repair Inhibiting Agents on R-loop Zone Localization and Abundance in U2OS Cells. (a) This live-cell image is an example of what live-cell images look like after activation of the catalytically inactive RNase H1. Green dots were termed “R-loop zones”. (b) 100 ng/mL of doxycycline was added 16 hours prior to drug treatment to induce HBD-EGFP expression (Olaparib was added at the same time as doxycycline). All other treatments were given for one hour. The count of total R-loop zones was

divided by number of cells counted for each treatment type. Almost all DNA damaging or DNA repair inhibiting drugs caused a likely increase in average R-loop zones. However, this experiment was only done once. Olaparib and Cisplatin show the largest average likely increase in R-loop zones per cell. Error bars indicate mean with SEM, while *p*-value was calculated using a one-way ANOVA test with multiple comparisons. Only Olaparib and Cisplatin showed significance.

6a

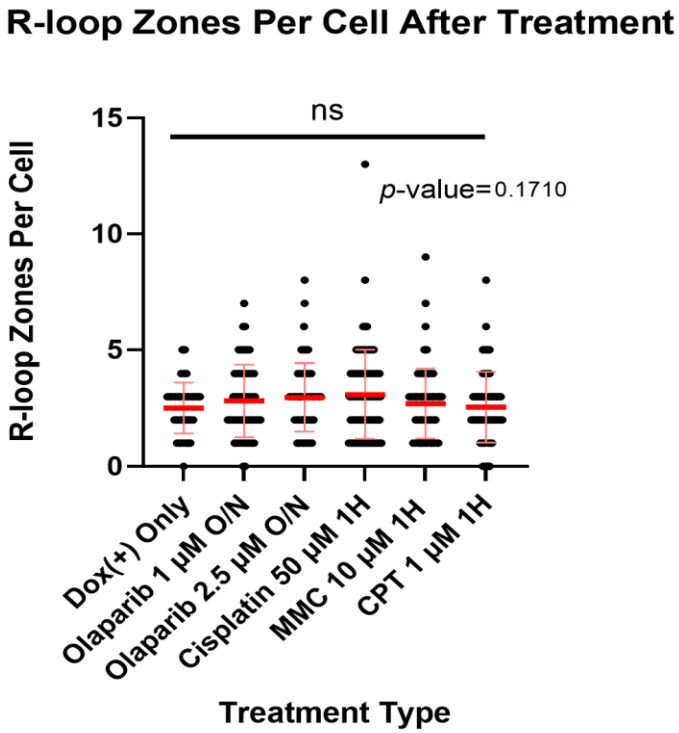

6b

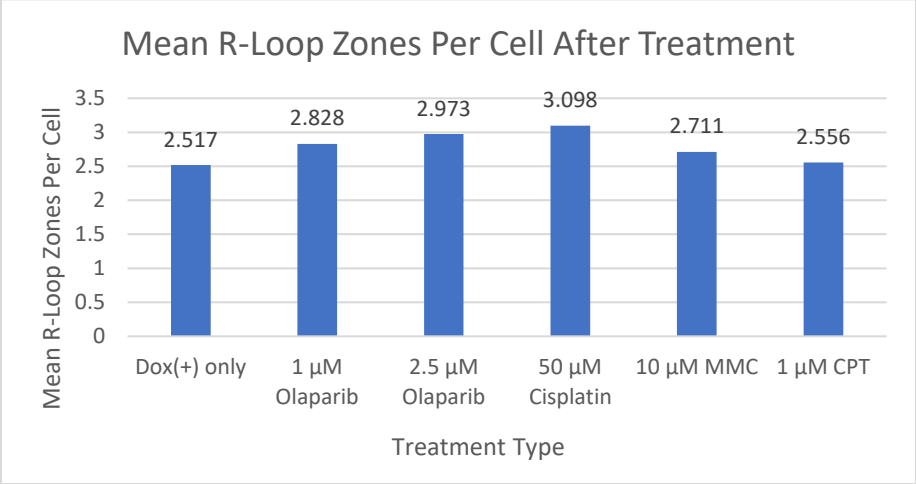

Figure 6: Average R-loop Zones Per Treatment Counted Using Imaris Software. (a) This graph shows Imaris 8.0.2 analyzation of R-loop Zones per HBD-EGFP U2OS cell after drug treatments. Not the average. Identical experiments were done a total of 3 times. Error bars indicate mean with SEM. P value calculated using a one-way ANOVA test. (b) This graph is the mean of all three drug treatments (the number above each bar graph) from Figure 6a to allow an easier comparison to 5b which was the average R-loop zones per cell. Similar trend seen as in Figure 5b. 100 ng/mL of doxycycline was added 16 hours prior to drug treatment to induce HBD-EGFP expression (Olaparib was added at the same time as doxycycline). All other treatments were for one hour.

In Figures 5b and 6, a trend was observed in which most of the chemotherapeutic agents likely increased the average number of R-loop zones per cell, regardless of analysis method. However, statistical significance was only seen between Olaparib and Cisplatin in one experimental test. This is not enough data to confirm if these chemotherapeutic agents increase R-loop numbers in cells, but the trend points towards a likely increase. In both Figures 5b and 6, the count of R-loop zones was done to determine if chemotherapeutic drugs influenced the number of R-loop zones. The data indicated that a 16-hour treatment of 2.5 µM Olaparib, a 1-hour treatment of 50 µM Cisplatin, and a 1-hour treatment of 10 µM MMC caused the largest average increase with most chemotherapeutic agents causing an increase in average R-loop zones per cell.

Overall, this chapter was important in aiding the future directions and goals of the project. It was determined that R-loop locations remain consistently in large fluorescent dots inside the nucleus. It was vital in determining that DNA damaging and DNA repair inhibiting chemotherapeutic agents likely increase R-loops inside cells. Showing this using multiple R-loop detection methods increases confidence in these results. This raises the possibility that an increase in R-loops may be an understudied reason for the drugs' success against cancer. It also allowed for overnight treatment of 2.5 μM Olaparib and a one-hour treatment of 50 μM Cisplatin to be used in future experiments to reliably increase R-loops inside of cells.

II. DETERMIINE WHETHER R-LOOPS ARE ENRICHED IN THE NUCLEOLUS AND WHETHER INCREASING THE ABUNDANCE OF R-LOOPS CAN ACTIVATE THE NUCLEOLAR STRESS PATHWAY

As previously mentioned in the background, the nucleolus is the site of ribosome biogenesis in cells and requires up to 80% of a cells energetic demands [4]. It has been shown in previous literature that nucleolar stress causes a translocation of proteins inside the nucleolus to the nucleoplasm, leading to activation of tumor suppressor p53 [8]. Known nucleolar stressors include hypoxia, UV, heat, nutrient starvation, DNA damage, and viral proteins [78].

R-loop zones imaged in live cell-imaging then prompted us to hypothesize that nuclear R-loops were mainly localized in the nucleolus. To test this, an immunofluorescence experiment was performed to determine if nucleolin and HBD-EGFP (R-loops) are within the same proximity. HBD-EGFP-U2OS cells were given doxycycline, fixed, and stained with the anti-nucleolin antibody. Nucleolin is a protein primarily located in the nucleolus, making it a useful marker of nucleoli locations [92]. Images in Figure 7 show a clear co-localization of R-loops to the nucleolus. This indicates that R-loops are concentrated in the nucleolus and further experiments regarding the effect of R-loops on the nucleolus could be examined.

7a

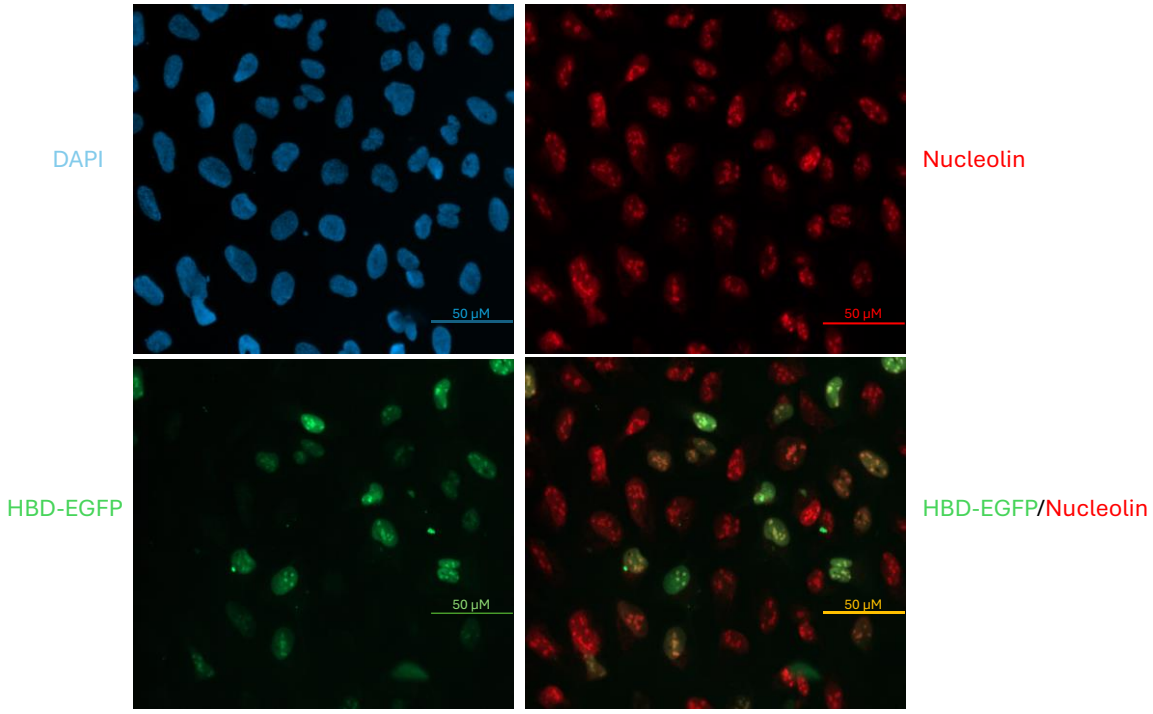

7b

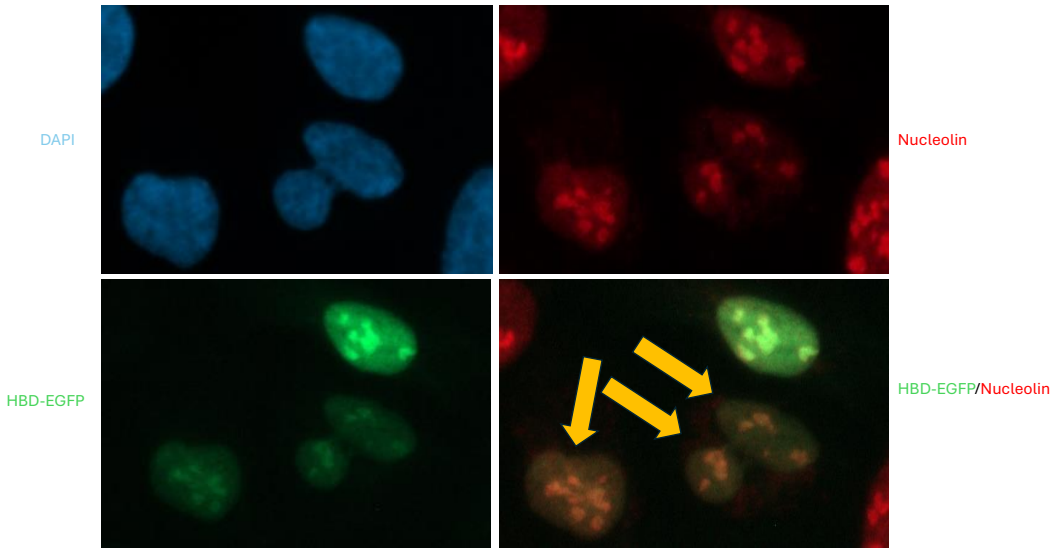

Figure 7: Immunofluorescence Showing R-Loop Localization in the Nucleolus. (a) Cells shown are HBD-EGFP-U2OS cells. This image shows each channel of the immunofluorescence

image. The bottom right channel is a merged image of HBD-EGFP cells and nucleolin showing a distinct co-localization of HBD-EGFP (R-loops) to nucleolin (nucleolus) without drug treatment. (b) Enlarged image of each channel in the immunofluorescence image. The bottom right channel is a merged image of HBD-EGFP/ nucleolin channel showing the co-localization between R-loops and nucleolin.

I then hypothesized that R-loop increases could induce nucleolar stress. The potent RNA:DNA helicase SETX was chosen to be knocked down in cells, which has been shown to increase R-loop levels in cells when SETX abundance is lower [73].

The results of the SETX knockdown was validated by western blotting (Figure 8a). A dot blot was performed to confirm an increase in R-loops after SETX knockdown (Figure 8b).

8a

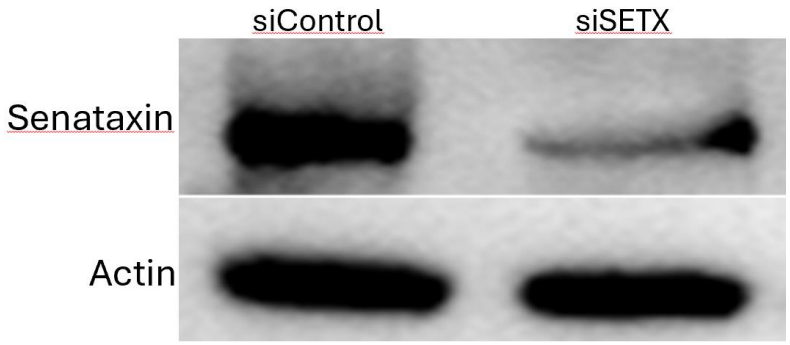

8b

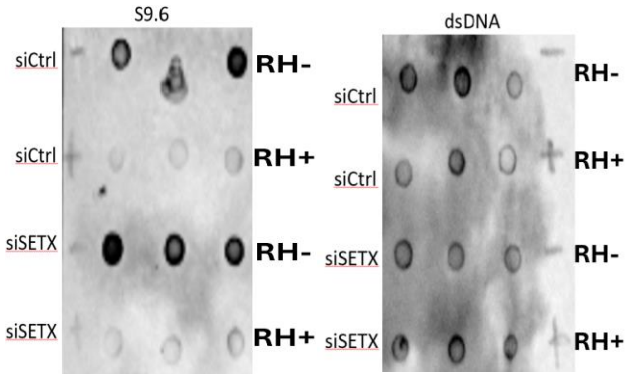

8c

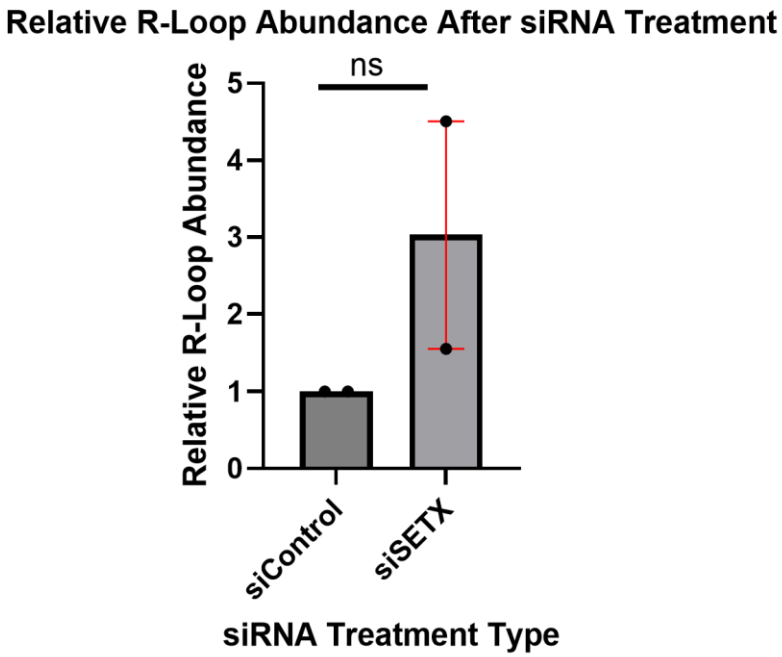

Figure 8: Knockdown of SETX Likely Increases R-Loops. (a) Western blot showing successful knockdown of SETX. (b) Dot blot membrane showing dsDNA and S9.6 (R-loop) dot intensity with the graph showing the dot blots relative abundance of R-loops after accounting for S9.6 non-specific binding. Fluorescence intensity normalized to no drug treatment. The graph from two different SETX knockdowns. Data non-significant due to not enough data. Likely increase in R-loops after SETX knockdown but could not be confirmed. Error bars are of mean with SEM.

It appears there was a probable increase in R-loops after SETX knockdown (Figure 8b). Next, I analyzed if nucleolar stress was induced by an increase in R-loops. A common way of assessing nucleolar stress is through the visualization of translocated nucleolar proteins out of the nucleolus [78]. Well-studied nucleolar proteins that translocate under nucleolar stress are NPM1 and fibrillarin. Fibrillarin, under nucleolar stress, will form rings or caps around the nucleolus while NPM1 will translocate to the nucleoplasm from the nucleolus [78]. This is when NPM1 is sequestering p53 ubiquitinases, allowing p53 levels to increase in cells. To visualize the

translocation of NPM1 and fibrillarin, which would indicate nucleolar stress, an immunofluorescence was performed. Two controls were introduced in the imaging. One control was siControl cells given Actinomycin D to induce nucleolar stress. At low concentrations <10 nM, Act. D acts as a potent RNA Polymerase I inhibitor causing nucleolar stress [93]. This was done to verify what should be seen in a cell that has activated the nucleolar stress pathway. Another control was untreated siControl cells, with lower R-loop levels relative to siSETX cells, to visualize nucleolar proteins in cells that have not activated the nucleolar stress pathway. Cells were fixed and stained with antibodies probing for NPM1 and fibrillarin and then imaging was carried out (Figure 9).

9a

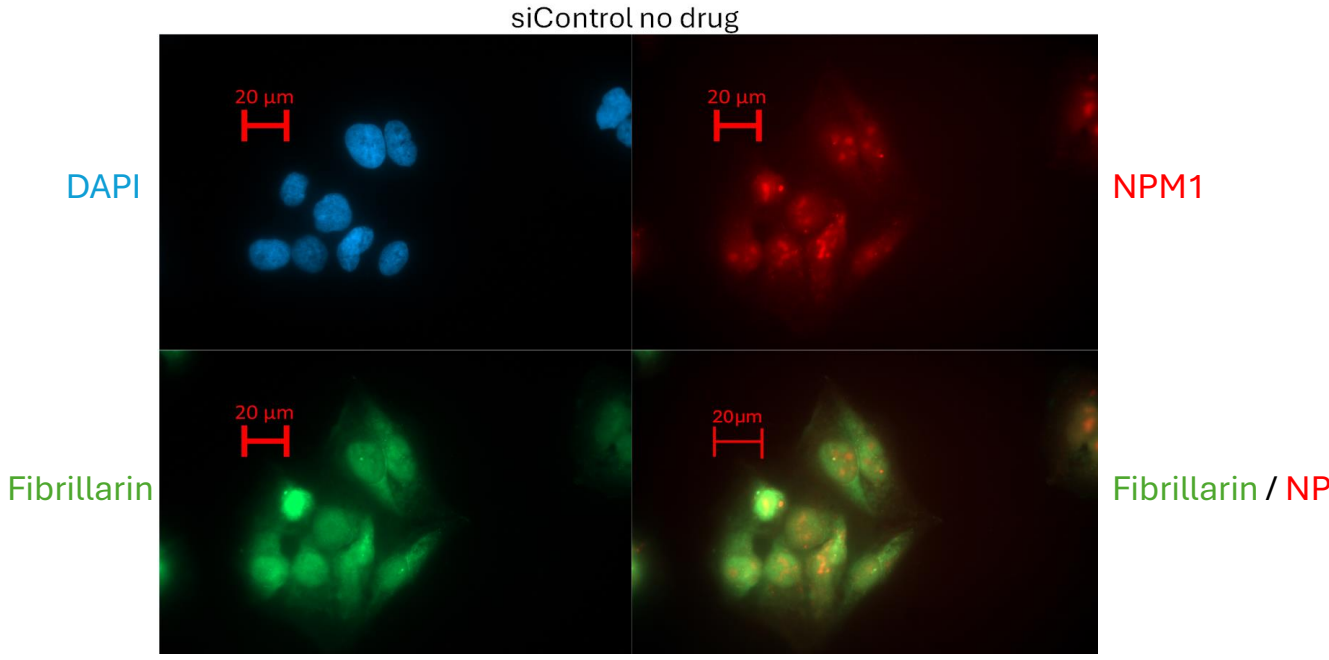

9b

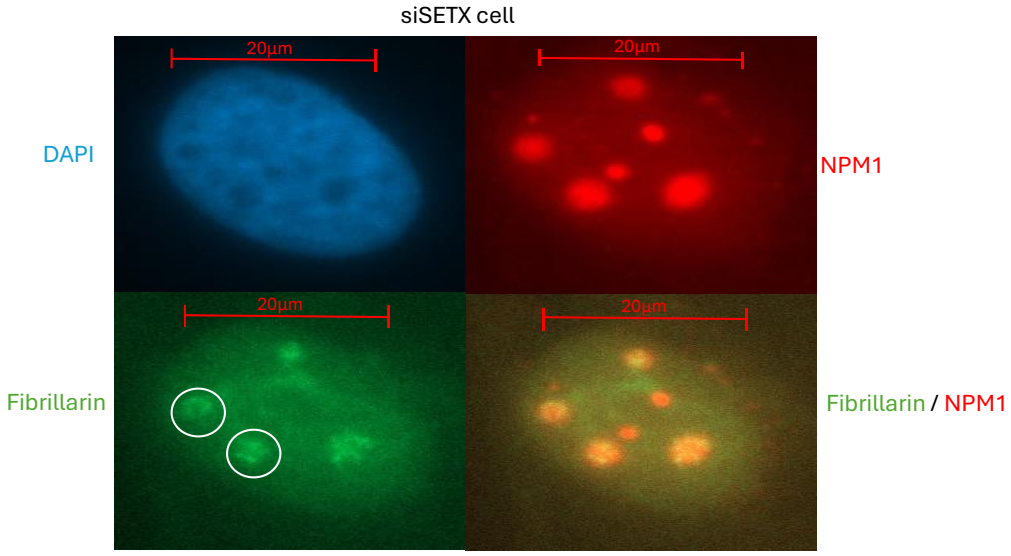
siSETX cell
DAPI
NPM1
Fibrillarin
Fibrillarin / NPM1
20µm
20µm
20µm
20µm

9c

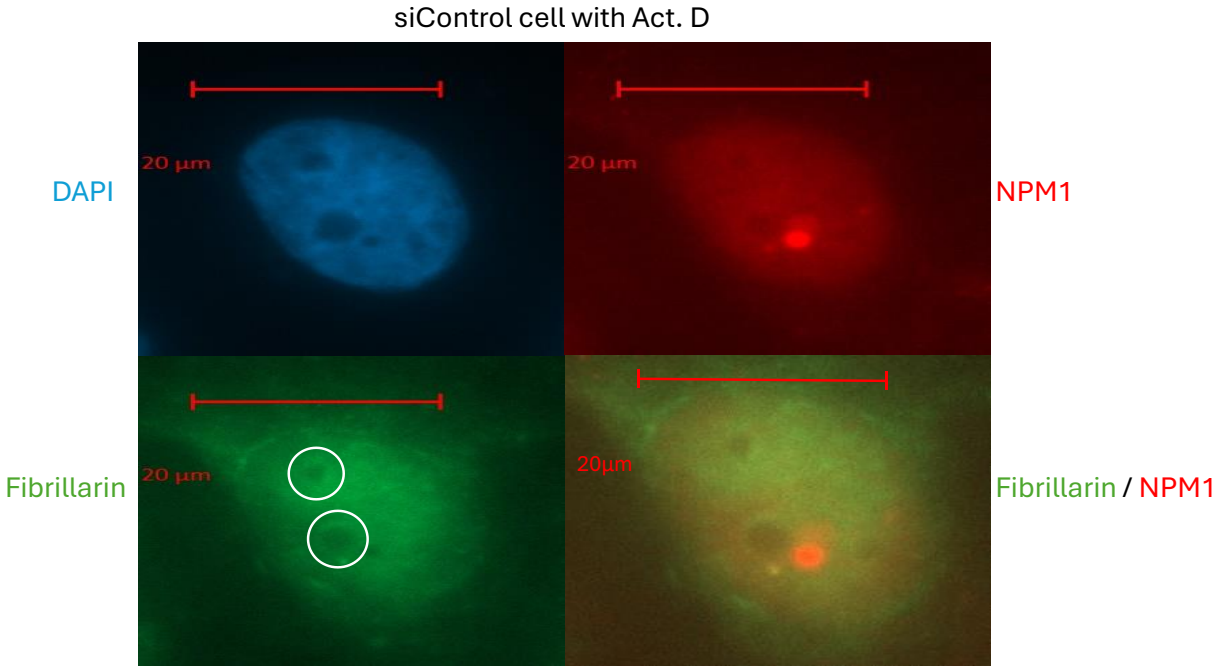
siControl cell with Act. D
DAPI
NPM1
Fibrillarin
Fibrillarin / NPM1
20 µm
20 µm
20 µm
20µm

Figure 9: Fibrillarin Rings Seen in Cells with Partial SETX Knockdown. (a) siControl cells with no increase in R-loops showing typical staining pattern of fibrillarin and NPM1. No nucleolar stress seen. (b) siSETX cells showing fibrillarin caps after an increase in R-loops. Fibrillarin caps are circled. Clear sign of nucleolar stress in Fibrillarin, however, NPM1 did not appear to translocate into the nucleoplasm as much as expected. Nucleolar stress pathway likely partially activated. (c) siControl cells given 8 nM of Act. D for 4 hours to induce nucleolar stress. Fibrillarin cap seen and circled. A translocation of NPM1 into the nucleoplasm is also seen. Nucleolar stress seen. Nucleolar stress pathway likely activated (9b).

The results from Figure 9 suggest that cells with an increase in R-loops have activated the nucleolar stress pathway. Figure 9a shows no clear concentration of fibrillarin along with NPM1 concentrated in dots not throughout the nucleoplasm. This is what is expected in a cell with no nucleolar stress pathway activation. Translocation of fibrillarin into caps/donut shapes outside of the nucleolus were seen in siSETX cells (Figure 9b). This is a clear sign of the activation of the nucleolar stress pathway. However, NPM1 did not appear to translocate into the nucleoplasm. It is possible that the nucleolar stress pathway was partially activated. Fibrillarin in Figure 9b and 9c both appear similar further indicating the activation of the nucleolar stress pathway in siSETX cells. This further indicates the activation of the nucleolar stress pathway in siSETX cells because cells in Figure 9c were given Actinomycin D. which acted as a positive control for nucleolar stress.

To further test if the nucleolar stress pathway was activated after an increase in nuclear R-loops, abundance of p53 needed to be determined. As previously mentioned, after the nucleolar stress pathway has been activated, an increase in p53 is seen in the cell due to the translocation of nucleolar proteins' sequestering of p53 ubiquitinase HDM2. This allows p53 levels to increase relative to cells that have not activated the nucleolar stress pathway. To

determine if p53 levels were increased after an increase in nuclear R-loops, a western blot was performed probing for p53 after SETX knockdown (Figure 10).

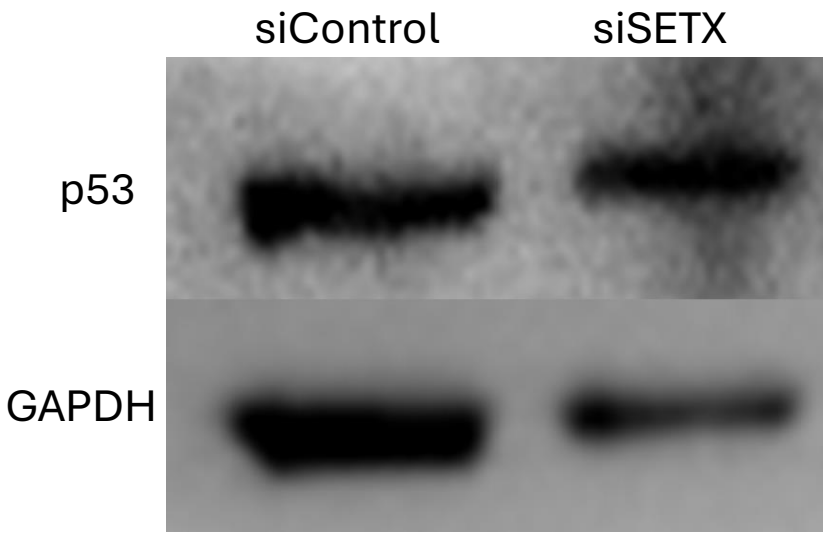

Figure 10: SETX Knockdown Elevates p53 Expression in Cells. The results from the western blot indicate an increase of p53 in siSETX cells when compared to siControl cells. These results add evidence that the nucleolar stress pathway was partially activated in cells with an increase in R-loops.

The results from the western blot indicate that in cells with an increase in R-loops, an increase in p53 is seen when compared to cells that have fewer R-loops. The western blot for p53, along with the immunofluorescence, adds increasing evidence that cells with an increase in R-loops are experiencing an activation of the nucleolar stress pathway.

III. DETERMINE WHETHER INCREASING R-LOOP ABUNDANCE DECREASES CELL VIABILITY

Next, it was questioned whether this increase of R-loops and possible activation of the nucleolar stress pathway could cause a change in cell viability. The objective of this chapter was to determine if increasing R-loops using the DNA damaging drug Cisplatin or DNA repair inhibiting drug Olaparib, combined with a knockdown of SETX, would cause R-loops to increase so much that cell viability would decrease. Based on previous experiments, knocking down SETX causes R-loops to likely increase (Figure 8), with cells effected showing signs that the nucleolar stress pathway was activated (Figures 9 and 10). Previous research also indicated adding DNA damaging or DNA repair inhibiting drugs increase R-loop abundance in cells (Figures 5 and 6). I hypothesized that by combining both R-loop increasing methods, cell viability would decrease in cancer cells. To perform this experiment, SETX needed to be knocked down with a siRNA transfection, and a western blot was required to show the knockdown (Appendix 1a). After that, a dot blot was required to ensure an R-loop increase occurred after the SETX knockdown (Appendix 1b). The quantification of R-loop abundance from this experiment was included in Figure 8.

Lastly, SETX knockdown and control cells were treated with either 16 hours of 2.5 μM Olaparib, 1 hour of 50 μM Cisplatin, or no drug treatment. Olaparib and Cisplatin were chosen as the drugs to be added to the cells due to their consistent and relatively large increase in R-loop

abundances compared to other chemotherapeutic agents tested (Figures 3, 5b, and 6). Cell viability was tested to determine if cell death had occurred more in cells with the highest increase in R-loops. This was done by seeding 10,000 cells per well in a 48 well plate for siSETX and siControl cells. The cells were stained with trypan blue and counted twice per well using a hematocytometer after addition of Olaparib, Cisplatin, or no drug treatment. Cells had to be seeded at only 10,000 cells per well due to a large number of cells needed for the western blot and dot blot in Appendix 1. The two cell counts per well were averaged and quantified to give an overall number of cells in the well (Figure 11).

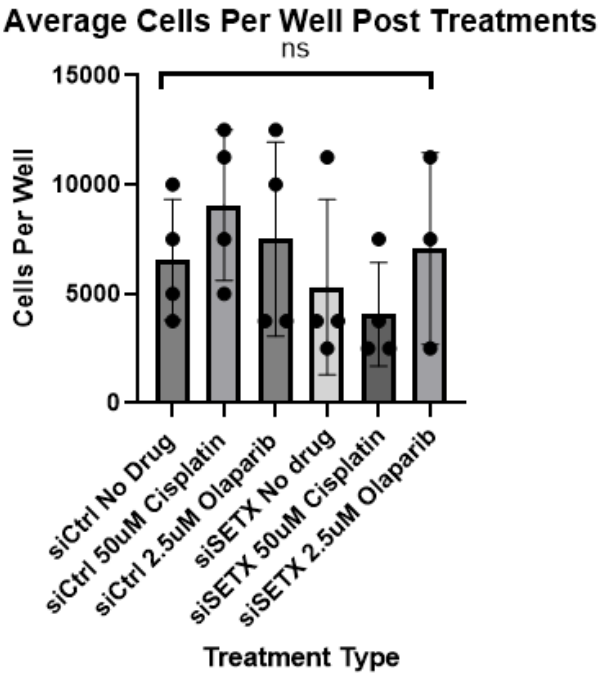

Figure 11: Cell Count Graph Showing No Clear Decrease After SETX siRNA Treatment with Olaparib, Cisplatin. The graph shows no consistent trend in cell viability with any treatment on the cells. Cells seeded at 10,000 cells per well in a 48 well plate. Four wells per treatment and each well counted twice with the average of the well graphed. Results compared to control are all non-significant. Error bars indicate mean with standard deviation.

The results show no clear connection or statistical significance between drug treatments or cells with a knockdown in SETX. It is likely that the results are inaccurate, and the method chosen to count cells did not work. Additionally, 10,000 cells were seeded in each cell making the results more inaccurate due to the cell count being below 10,000 for siControl and no drug treatment cells. It is possible that using such a small initial seeding of cells and a relatively inaccurate counting method contributed to the results in Figure 11. Unfortunately, no conclusions can be gathered from the cell viability data.

CHAPTER FOUR

DISCUSSION

The study of R-loops and their relationship with nucleolar stress has been understudied and many mysteries remain about the relationship between R-loops and nucleolar stress. The aim of this manuscript was to gain an insight on the possibility that R-loops could be a source of nucleolar stress, and that increasing R-loops in cells could be a way to kill cancer cells. The data indicated that several DNA damage inducing or DNA repair inhibiting drugs likely increase R-loop levels, and this could be an understudied impact on their effectiveness as successful chemotherapeutic agents (Figures 3, 5, and 6). This was also determined using multiple different mechanisms, further increasing the reliability of the results.

The immunofluorescence results show the co-localization between R-loops and nucleolin (Figure 7), suggesting that R-loops are heavily concentrated in the nucleolus. Figure 7 results indicate that the nucleolus and R-loops may contain a valuable interaction to a cells success. This allows for the possibility of all kinds of discoveries to be made regarding the connection between R-loops and the nucleolus. By showing that depletion of Senataxin likely causes an increase in R-loops (Figure 8), this confirmed literature data and showed that knocking down Senataxin could be used to artificially increase R-loops in cells. This result also showcases the effectiveness of SETX as an RNA:DNA helicase. The Immunofluorescence staining of NPM1 and fibrillarin had important impacts on this manuscript. Under conditions with increased R-loops in cells due to the SETX knockdown fibrillarin caps were seen, indicating an activation of

the nucleolar stress pathway (Figure 9). This was a promising result suggesting the nucleolar stress pathway was activated in cells that had an increase in R-loops from a SETX knockdown. However, the lack of translocation of the nucleolus into the nucleoplasm was not evident. This meant the immunofluorescence data could not confirm if the nucleolar stress pathway was activated. Luckily, there was another way to test if the nucleolar stress pathway had been activated. The other method for detecting if there was activation of the nucleolar stress was to test for p53 abundance. By comparing p53 abundance in cells that had a knockdown of SETX versus cells that did not it was possible to gain a better insight. The data from the p53 western blot confirmed an increase in p53 in cells with more R-loops (Figure 10). This led to the conclusion that knocking down SETX can cause a likely activation of the nucleolar stress pathway, but due to the NPM1 data it may not have been a complete activation. Lastly, it was necessary to test for changes in cell viability in cells with a combination of the two methods that increase R-loops. The two methods were adding DNA damage inducing or DNA repair inhibiting drugs, which likely increased R-loop levels in cells, with a knockdown of SETX to further increase R-loop levels in cells. This experiment yielded no meaningful result (Figure 11).

There were experiments that could have been done in a better way. For example, imaging data could have been quantified in a better way, specifically NPM1 translocation from the nucleolus to the nucleoplasm. Next, the S9.6 antibody is one of the most accurate antibodies at detecting R-loops in cells; however, it is not perfect and does recognize other genomic products besides R-loops. This causes the results to be more difficult to reproduce, making the results more questionable. Also, the cell viability assay failed, likely due to the small number of cells

that were originally seeded and poor method of choice to count cells. It is unfortunate that a clear result could not be obtained from the cell viability data.

Future directions from this manuscript include knocking down different R-loop helicases to understand if that could cause signs of nucleolar stress. Considering SETX showed signs of being a potent RNA:DNA helicase, it would be useful to understand other proteins SETX interacts with to achieve R-loop resolution. It may also be useful to determine if decreasing R-loop abundance can activate the nucleolar stress pathway. Lastly, gaining insight on where in the genome R-loops increase after a SETX knockdown could be valuable information. This could be achieved using sequencing data.

To conclude, this manuscript determined that DNA damage inducing and DNA repair inhibiting chemotherapeutic drugs cause a likely increase in R-loops, R-loops are localized in the nucleus, a knockdown of SETX likely causes an increase in R-loops, this increase in R-loops is likely the cause of the translocation of nucleolar proteins such as fibrillarin, and an increase in R-loops can possibly increase levels of p53 in cells; likely due to the activation of the nucleolar stress pathway.

APPENDIX

Additional Data

1a

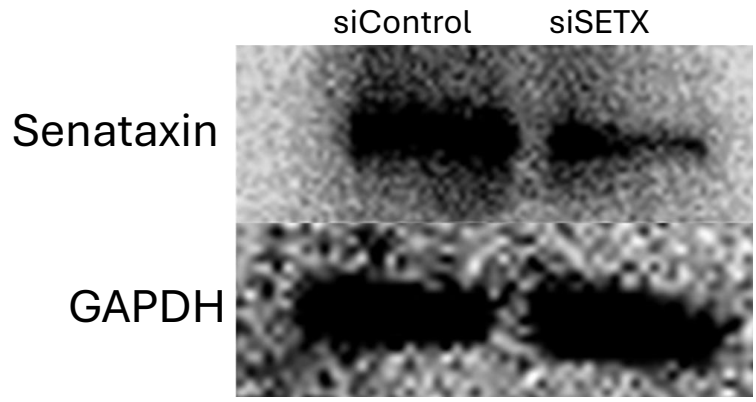

1b

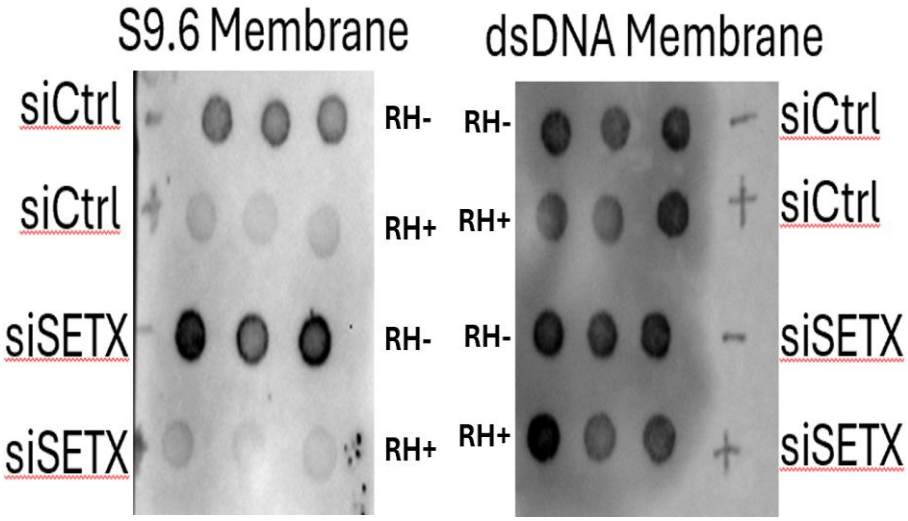

Figure 1: SETX Knockdown and Corresponding Dot Blot Membrane. (a) SETX Membrane is shown indicating decreased levels of SETX in siSETX cells after siRNA transfection. (b) Dot blot membrane showing fluorescence of the S9.6 antibody and dsDNA antibody on their membranes in siControl and siSETX cells. The data of quantified relative R-loop abundance from this dot blot was combined with the graph in Figure 8b.

REFERENCE LIST

1 Allison, D. F. & Wang, G. G. R-loops: formation, function, and relevance to cell stress. *Cell Stress* **3**, 38-46, doi:10.15698/cst2019.02.175 (2019).

2 Garcia-Muse, T. & Aguilera, A. R Loops: From Physiological to Pathological Roles. *Cell* **179**, 604-618, doi:10.1016/j.cell.2019.08.055 (2019).

3 Li, F. *et al.* R-Loops in Genome Instability and Cancer. *Cancers* **15**, 4986 (2023).

4 Dubois, M.-L. & Boisvert, F.-M. in *The Functional Nucleus* (eds David P. Bazett-Jones & Graham Dellaire) 29-49 (Springer International Publishing, 2016).

5 Pelletier, J., Thomas, G. & Volarević, S. Ribosome biogenesis in cancer: new players and therapeutic avenues. *Nature Reviews Cancer* **18**, 51-63, doi:10.1038/nrc.2017.104 (2018).

6 Donizy, P., Biecek, P., Halon, A., Maciejczyk, A. & Matkowski, R. Nucleoli cytomorphology in cutaneous melanoma cells - a new prognostic approach to an old concept. *Diagn Pathol* **12**, 88, doi:10.1186/s13000-017-0675-7 (2017).

7 Zink, D., Fischer, A. H. & Nickerson, J. A. Nuclear structure in cancer cells. *Nature Reviews Cancer* **4**, 677-687, doi:10.1038/nrc1430 (2004).

8 James, A., Wang, Y., Raje, H., Rosby, R. & DiMario, P. Nucleolar stress with and without p53. *Nucleus* **5**, 402-426, doi:10.4161/nucl.32235 (2014).

9 Petermann, E., Lan, L. & Zou, L. Sources, resolution and physiological relevance of R-loops and RNA–DNA hybrids. *Nature Reviews Molecular Cell Biology* **23**, 521-540, doi:10.1038/s41580-022-00474-x (2022).

10 Lam, F. C., Kong, Y. W. & Yaffe, M. B. Inducing DNA damage through R-loops to kill cancer cells. *Mol Cell Oncol* **8**, 1848233, doi:10.1080/23723556.2020.1848233 (2020).

11 Zatreanu, D. *et al.* Elongation Factor TFIIS Prevents Transcription Stress and R-Loop Accumulation to Maintain Genome Stability. *Mol Cell* **76**, 57-69 e59, doi:10.1016/j.molcel.2019.07.037 (2019).

12 Stirling, P. C. *et al.* R-loop-mediated genome instability in mRNA cleavage and polyadenylation mutants. *Genes Dev* **26**, 163-175, doi:10.1101/gad.179721.111 (2012).

13 Brickner, J. R., Garzon, J. L. & Cimprich, K. A. Walking a tightrope: The complex balancing act of R-loops in genome stability. *Mol Cell* **82**, 2267-2297, doi:10.1016/j.molcel.2022.04.014 (2022).

14 Kim, A. & Wang, G. G. R-loop and its functions at the regulatory interfaces between transcription and (epi)genome. *Biochim Biophys Acta Gene Regul Mech* **1864**, 194750, doi:10.1016/j.bbagrm.2021.194750 (2021).

15 Crossley, M. P., Bocek, M. J., Hamperl, S., Swigut, T. & Cimprich, K. A. qDRIP: a method to quantitatively assess RNA-DNA hybrid formation genome-wide. *Nucleic Acids Res* **48**, e84, doi:10.1093/nar/gkaa500 (2020).

16 Sanz, L. A. *et al.* Prevalent, Dynamic, and Conserved R-Loop Structures Associate with Specific Epigenomic Signatures in Mammals. *Mol Cell* **63**, 167-178, doi:10.1016/j.molcel.2016.05.032 (2016).

17 Liu, Q. *et al.* Emerging roles of centromeric RNAs in centromere formation and function. *Genes Genomics* **43**, 217-226, doi:10.1007/s13258-021-01041-y (2021).

18 Niehrs, C. & Luke, B. Regulatory R-loops as facilitators of gene expression and genome stability. *Nat Rev Mol Cell Biol* **21**, 167-178, doi:10.1038/s41580-019-0206-3 (2020).
19 Tan, J. & Lan, L. The DNA secondary structures at telomeres and genome instability. *Cell Biosci* **10**, 47, doi:10.1186/s13578-020-00409-z (2020).
20 Grunseich, C. *et al.* Senataxin Mutation Reveals How R-Loops Promote Transcription by Blocking DNA Methylation at Gene Promoters. *Mol Cell* **69**, 426-437.e427, doi:10.1016/j.molcel.2017.12.030 (2018).
21 Aguilera, A. & Gomez-Gonzalez, B. Genome instability: a mechanistic view of its causes and consequences. *Nat Rev Genet* **9**, 204-217, doi:10.1038/nrg2268 (2008).
22 Holt, I. J. The mitochondrial R-loop. *Nucleic Acids Research* **47**, 5480-5489, doi:10.1093/nar/gkz277 (2019).
23 Roy, D., Yu, K. & Lieber, M. R. Mechanism of R-loop formation at immunoglobulin class switch sequences. *Mol Cell Biol* **28**, 50-60, doi:10.1128/MCB.01251-07 (2008).
24 Duarte, J. H. Functional switching. *Nature Immunology* **17**, S12-S12, doi:10.1038/ni.3607 (2016).
25 Muramatsu, M. *et al.* Specific Expression of Activation-induced Cytidine Deaminase (AID), a Novel Member of the RNA-editing Deaminase Family in Germinal Center B Cells*. *Journal of Biological Chemistry* **274**, 18470-18476, doi:https://doi.org/10.1074/jbc.274.26.18470 (1999).
26 Bransteitter, R., Pham, P., Scharff, M. D. & Goodman, M. F. Activation-induced cytidine deaminase deaminates deoxycytidine on single-stranded DNA but requires the action of RNase. *Proc Natl Acad Sci U S A* **100**, 4102-4107, doi:10.1073/pnas.0730835100 (2003).
27 Huang, F. T., Yu, K., Hsieh, C. L. & Lieber, M. R. Downstream boundary of chromosomal R-loops at murine switch regions: implications for the mechanism of class switch recombination. *Proc Natl Acad Sci U S A* **103**, 5030-5035, doi:10.1073/pnas.0506548103 (2006).
28 Perez-Martinez, L., Ozturk, M., Butter, F. & Luke, B. Npl3 stabilizes R-loops at telomeres to prevent accelerated replicative senescence. *EMBO Rep* **21**, e49087, doi:10.15252/embr.201949087 (2020).
29 Chebly, A. *et al.* Telomeric Repeat-Containing RNA (TERRA): A Review of the Literature and First Assessment in Cutaneous T-Cell Lymphomas. *Genes (Basel)* **13**, doi:10.3390/genes13030539 (2022).
30 Yang, Y. *et al.* Arginine methylation facilitates the recruitment of TOP3B to chromatin to prevent R loop accumulation. *Mol Cell* **53**, 484-497, doi:10.1016/j.molcel.2014.01.011 (2014).
31 Gan, W. *et al.* R-loop-mediated genomic instability is caused by impairment of replication fork progression. *Genes Dev* **25**, 2041-2056, doi:10.1101/gad.17010011 (2011).
32 So, C. C. & Martin, A. DSB structure impacts DNA recombination leading to class switching and chromosomal translocations in human B cells. *PLoS Genet* **15**, e1008101, doi:10.1371/journal.pgen.1008101 (2019).
33 Elsakrmy, N. & Cui, H. R-Loops and R-Loop-Binding Proteins in Cancer Progression and Drug Resistance. *Int J Mol Sci* **24**, doi:10.3390/ijms24087064 (2023).
34 Hasanova, Z., Klapstova, V., Porrua, O., Stefl, R. & Sebesta, M. Human senataxin is a bona fide R-loop resolving enzyme and transcription termination factor. *Nucleic Acids Research* **51**, 2818-2837, doi:10.1093/nar/gkad092 (2023).
35 Chang, E. Y. *et al.* RECQ-like helicases Sgs1 and BLM regulate R-loop-associated genome instability. *J Cell Biol* **216**, 3991-4005, doi:10.1083/jcb.201703168 (2017).
36 Song, C., Hotz-Wagenblatt, A., Voit, R. & Grummt, I. SIRT7 and the DEAD-box helicase DDX21 cooperate to resolve genomic R loops and safeguard genome stability. *Genes Dev* **31**, 1370-1381, doi:10.1101/gad.300624.117 (2017).

37 Mersaoui, S. Y. *et al.* Arginine methylation of the DDX5 helicase RGG/RG motif by PRMT5 regulates resolution of RNA:DNA hybrids. *EMBO J* **38**, e100986, doi:10.15252/embj.2018100986 (2019).
38 Pruss, G. J., Manes, S. H. & Drlica, K. Escherichia coli DNA topoisomerase I mutants: Increased supercoiling is corrected by mutations near gyrase genes. *Cell* **31**, 35-42, doi:https://doi.org/10.1016/0092-8674(82)90402-0 (1982).
39 Cerritelli, S. M. & Crouch, R. J. Ribonuclease H: the enzymes in eukaryotes. *Febs j* **276**, 1494-1505, doi:10.1111/j.1742-4658.2009.06908.x (2009).
40 Lockhart, A. *et al.* RNase H1 and H2 Are Differentially Regulated to Process RNA-DNA Hybrids. *Cell Rep* **29**, 2890-2900 e2895, doi:10.1016/j.celrep.2019.10.108 (2019).
41 Hyjek, M., Figiel, M. & Nowotny, M. RNases H: Structure and mechanism. *DNA Repair (Amst)* **84**, 102672, doi:10.1016/j.dnarep.2019.102672 (2019).
42 Crow, Y. J. *et al.* Mutations in genes encoding ribonuclease H2 subunits cause Aicardi-Goutieres syndrome and mimic congenital viral brain infection. *Nat Genet* **38**, 910-916, doi:10.1038/ng1842 (2006).
43 Lin, R. *et al.* R-loopBase: a knowledgebase for genome-wide R-loop formation and regulation. *Nucleic Acids Research* **50**, D303-D315, doi:10.1093/nar/gkab1103 (2021).
44 Sabino, J. C. *et al.* Epigenetic reprogramming by TET enzymes impacts co-transcriptional R-loops. *eLife* **11**, e69476, doi:10.7554/eLife.69476 (2022).
45 Bulut-Karslioglu, A. *et al.* Inhibition of mTOR induces a paused pluripotent state. *Nature* **540**, 119-123, doi:10.1038/nature20578 (2016).
46 Moore, L. D., Le, T. & Fan, G. DNA Methylation and Its Basic Function. *Neuropsychopharmacology* **38**, 23-38, doi:10.1038/npp.2012.112 (2013).
47 Ginno, P. A., Lott, P. L., Christensen, H. C., Korf, I. & Chedin, F. R-loop formation is a distinctive characteristic of unmethylated human CpG island promoters. *Mol Cell* **45**, 814-825, doi:10.1016/j.molcel.2012.01.017 (2012).
48 Chédin, F., Hartono, S. R., Sanz, L. A. & Vanoosthuyse, V. Best practices for the visualization, mapping, and manipulation of R-loops. *The EMBO Journal* **40**, e106394, doi:https://doi.org/10.15252/embj.2020106394 (2021).
49 Konig, F., Schubert, T. & Langst, G. The monoclonal S9.6 antibody exhibits highly variable binding affinities towards different R-loop sequences. *PLoS One* **12**, e0178875, doi:10.1371/journal.pone.0178875 (2017).
50 Hartono, S. R. *et al.* The Affinity of the S9.6 Antibody for Double-Stranded RNAs Impacts the Accurate Mapping of R-Loops in Fission Yeast. *J Mol Biol* **430**, 272-284, doi:10.1016/j.jmb.2017.12.016 (2018).
51 Wu, H., Lima, W. F. & Crooke, S. T. Investigating the structure of human RNase H1 by site-directed mutagenesis. *J Biol Chem* **276**, 23547-23553, doi:10.1074/jbc.M009676200 (2001).
52 Chen, L. *et al.* R-ChIP Using Inactive RNase H Reveals Dynamic Coupling of R-loops with Transcriptional Pausing at Gene Promoters. *Mol Cell* **68**, 745-757 e745, doi:10.1016/j.molcel.2017.10.008 (2017).
53 Malig, M., Hartono, S. R., Giafaglione, J. M., Sanz, L. A. & Chedin, F. Ultra-deep Coverage Single-molecule R-loop Footprinting Reveals Principles of R-loop Formation. *J Mol Biol* **432**, 2271-2288, doi:10.1016/j.jmb.2020.02.014 (2020).
54 Yu, K., Chedin, F., Hsieh, C.-L., Wilson, T. E. & Lieber, M. R. R-loops at immunoglobulin class switch regions in the chromosomes of stimulated B cells. *Nature Immunology* **4**, 442-451, doi:10.1038/ni919 (2003).
55 Gao, J. *et al.* Toward an understanding of the detection and function of R-loops in plants. *Journal of Experimental Botany* **72**, 6110-6122, doi:10.1093/jxb/erab280 (2021).

56 Wahba, L., Costantino, L., Tan, F. J., Zimmer, A. & Koshland, D. S1-DRIP-seq identifies high expression and polyA tracts as major contributors to R-loop formation. *Genes Dev* **30**, 1327-1338, doi:10.1101/gad.280834.116 (2016).
57 Raghavan, S. C., Tsai, A., Hsieh, C. L. & Lieber, M. R. Analysis of non-B DNA structure at chromosomal sites in the mammalian genome. *Methods Enzymol* **409**, 301-316, doi:10.1016/S0076-6879(05)09017-8 (2006).
58 Gentry, M. & Hennig, L. A Structural Bisulfite Assay to Identify DNA Cruciforms. *Mol Plant* **9**, 1328-1336, doi:10.1016/j.molp.2016.06.003 (2016).
59 Amparo, C. *et al.* Duplex DNA from Sites of Helicase-Polymerase Uncoupling Links Non-B DNA Structure Formation to Replicative Stress. *Cancer Genomics Proteomics* **17**, 101-115, doi:10.21873/cgp.20171 (2020).
60 Gorthi, A. *et al.* EWS-FLI1 increases transcription to cause R-loops and block BRCA1 repair in Ewing sarcoma. *Nature* **555**, 387-391, doi:10.1038/nature25748 (2018).
61 Turc-Carel, C., Philip, I., Berger, M. P., Philip, T. & Lenoir, G. M. Chromosome study of Ewing's sarcoma (ES) cell lines. Consistency of a reciprocal translocation t(11;22)(q24;q12). *Cancer Genet Cytogenet* **12**, 1-19, doi:10.1016/0165-4608(84)90002-5 (1984).
62 Chiang, H. C. *et al.* BRCA1-associated R-loop affects transcription and differentiation in breast luminal epithelial cells. *Nucleic Acids Res* **47**, 5086-5099, doi:10.1093/nar/gkz262 (2019).
63 Hatchi, E. *et al.* BRCA1 recruitment to transcriptional pause sites is required for R-loop-driven DNA damage repair. *Mol Cell* **57**, 636-647, doi:10.1016/j.molcel.2015.01.011 (2015).
64 Luo, H. *et al.* HOTTIP-dependent R-loop formation regulates CTCF boundary activity and TAD integrity in leukemia. *Mol Cell* **82**, 833-851 e811, doi:10.1016/j.molcel.2022.01.014 (2022).
65 De Magis, A. *et al.* DNA damage and genome instability by G-quadruplex ligands are mediated by R loops in human cancer cells. *Proc Natl Acad Sci U S A* **116**, 816-825, doi:10.1073/pnas.1810409116 (2019).
66 Aguilera, A. & Garcia-Muse, T. R loops: from transcription byproducts to threats to genome stability. *Mol Cell* **46**, 115-124, doi:10.1016/j.molcel.2012.04.009 (2012).
67 Skourti-Stathaki, K. & Proudfoot, N. J. A double-edged sword: R loops as threats to genome integrity and powerful regulators of gene expression. *Genes Dev* **28**, 1384-1396, doi:10.1101/gad.242990.114 (2014).
68 Belkina, A. C. & Denis, G. V. BET domain co-regulators in obesity, inflammation and cancer. *Nat Rev Cancer* **12**, 465-477, doi:10.1038/nrc3256 (2012).
69 Chiang, C. M. Brd4 engagement from chromatin targeting to transcriptional regulation: selective contact with acetylated histone H3 and H4. *F1000 Biol Rep* **1**, 98, doi:10.3410/B1-98 (2009).
70 Zuber, J. *et al.* RNAi screen identifies Brd4 as a therapeutic target in acute myeloid leukaemia. *Nature* **478**, 524-528, doi:10.1038/nature10334 (2011).
71 Chapuy, B. *et al.* Discovery and characterization of super-enhancer-associated dependencies in diffuse large B cell lymphoma. *Cancer Cell* **24**, 777-790, doi:10.1016/j.ccr.2013.11.003 (2013).
72 Shu, S. *et al.* Response and resistance to BET bromodomain inhibitors in triple-negative breast cancer. *Nature* **529**, 413-417, doi:10.1038/nature16508 (2016).
73 Hasanova, Z., Klapstova, V., Porrua, O., Stefl, R. & Sebesta, M. Human senataxin is a bona fide R-loop resolving enzyme and transcription termination factor. *Nucleic Acids Res* **51**, 2818-2837, doi:10.1093/nar/gkad092 (2023).
74 Gatti, V., De Domenico, S., Melino, G. & Peschiaroli, A. Senataxin and R-loops homeostasis: multifaced implications in carcinogenesis. *Cell Death Discov* **9**, 145, doi:10.1038/s41420-023-01441-x (2023).
75 Sollier, J. *et al.* Transcription-coupled nucleotide excision repair factors promote R-loop-induced genome instability. *Mol Cell* **56**, 777-785, doi:10.1016/j.molcel.2014.10.020 (2014).

76 Lafita-Navarro, M. C. & Conacci-Sorrell, M. Nucleolar stress: From development to cancer. *Semin Cell Dev Biol* **136**, 64-74, doi:10.1016/j.semcdb.2022.04.001 (2023).
77 Rubbi, C. P. & Milner, J. Disruption of the nucleolus mediates stabilization of p53 in response to DNA damage and other stresses. *Embo j* **22**, 6068-6077, doi:10.1093/emboj/cdg579 (2003).
78 Yang, K., Yang, J. & Yi, J. Nucleolar Stress: hallmarks, sensing mechanism and diseases. *Cell Stress* **2**, 125-140, doi:10.15698/cst2018.06.139 (2018).
79 Denko, N. *et al.* Hypoxia actively represses transcription by inducing negative cofactor 2 (Dr1/DrAP1) and blocking preinitiation complex assembly. *J Biol Chem* **278**, 5744-5749, doi:10.1074/jbc.M212534200 (2003).
80 Brooks, C. L. & Gu, W. p53 ubiquitination: Mdm2 and beyond. *Mol Cell* **21**, 307-315, doi:10.1016/j.molcel.2006.01.020 (2006).
81 Hafner, A., Bulyk, M. L., Jambhekar, A. & Lahav, G. The multiple mechanisms that regulate p53 activity and cell fate. *Nat Rev Mol Cell Biol* **20**, 199-210, doi:10.1038/s41580-019-0110-x (2019).
82 Box, J. K. *et al.* Nucleophosmin: from structure and function to disease development. *BMC Molecular Biology* **17**, 19, doi:10.1186/s12867-016-0073-9 (2016).
83 Burger, K. *et al.* Chemotherapeutic drugs inhibit ribosome biogenesis at various levels. *J Biol Chem* **285**, 12416-12425, doi:10.1074/jbc.M109.074211 (2010).
84 Zheng, J. *et al.* Structure of human MDM2 complexed with RPL11 reveals the molecular basis of p53 activation. *Genes Dev* **29**, 1524-1534, doi:10.1101/gad.261792.115 (2015).
85 Bieging, K. T., Mello, S. S. & Attardi, L. D. Unravelling mechanisms of p53-mediated tumour suppression. *Nat Rev Cancer* **14**, 359-370, doi:10.1038/nrc3711 (2014).
86 Pereira-Santana, A. *et al.* Fibrillarin evolution through the Tree of Life: Comparative genomics and microsynteny network analyses provide new insights into the evolutionary history of Fibrillarin. *PLoS Comput Biol* **16**, e1008318, doi:10.1371/journal.pcbi.1008318 (2020).
87 Decle-Carrasco, S., Rodríguez-Piña, A. L., Rodríguez-Zapata, L. C. & Castano, E. Current research on viral proteins that interact with fibrillarin. *Mol Biol Rep* **50**, 4631-4643, doi:10.1007/s11033-023-08343-2 (2023).
88 Rodriguez-Corona, U., Sobol, M., Rodriguez-Zapata, L. C., Hozak, P. & Castano, E. Fibrillarin from Archaea to human. *Biol Cell* **107**, 159-174, doi:10.1111/boc.201400077 (2015).
89 Potapova, T. A. *et al.* Distinct states of nucleolar stress induced by anticancer drugs. *eLife* **12**, RP88799, doi:10.7554/eLife.88799 (2023).
90 Chen, C. S. *et al.* AKT mediates actinomycin D-induced p53 expression. *Oncotarget* **5**, 693-703, doi:10.18632/oncotarget.1328 (2014).
91 Dowling, J. W., Smith, J. R. & Forero, A. Protocol for detection of in vitro R-loop formation using dot blots. *STAR Protocols* **5**, 102857, doi:https://doi.org/10.1016/j.xpro.2024.102857 (2024).
92 Abdelmohsen, K. & Gorospe, M. RNA-binding protein nucleolin in disease. *RNA Biol* **9**, 799-808, doi:10.4161/rna.19718 (2012).
93 Liang, Y. X. *et al.* Nucleolar stress regulates stromal-epithelial transition via NPM1 during decidualization. *Reproduction* **160**, 491-500, doi:10.1530/rep-20-0051 (2020).

VITA

The author, Kevin J. Shane, was born on April 23, 2000, in Mount Prospect, Illinois. He is the youngest of three children born to John Shane and Maureen Meersman. Kevin attended Prospect High School in Mount Prospect, Illinois where he graduated in 2018. He then went on to attend the University of Denver in Denver, CO, obtaining a Bachelor of Science degree in molecular biology along with minors in chemistry and physics. After graduating from University of Denver he returned to the Chicagoland area and began a master's program at Loyola University in August of 2022. He joined the ICB (integrative cellular biology) program and went on to join the Chai lab. The Chai lab researches DNA replication and repair which led him to focus on the role of R-loops and their connection to nucleolar stress.